of PEDF-stimulated NSCs with low levels of Notch signaling to proliferate and generate multiple cell types.

Andreu-Agulló *et al.*[7] have thus elucidated the pathways used by PEDF to regulate adult periventricular NSC function. The identity of the receptor that initiates PEDF signaling, however, remains unknown. Pharmacological inhibition of the only known putative PEDF receptor, adipose triglyceride lipase[11], did not affect PEDF actions on adult periventricular NSCs. If expression of the PEDF receptor is restricted to adult periventricular NSCs, its use as a prospective marker would substantially aid in their study.

The interpretation of PEDF's role in regulating adult NSC function, however, could depend on which population of label-retaining cells one selects as the 'true' stem cell. Presuming that NSCs with high levels of Notch signaling and EGFR are at the top of the hierarchy might mean that PEDF functions to extend the cell-generating capacity of NSCs with low levels of Notch signaling (**Fig. 1a**). Alternatively, one could assume that label-retaining cells with low Notch signaling and EGFR expression are the quiescent NSCs at the top of the hierarchy; in this case, PEDF would function to activate them (**Fig. 2**). Indeed, intraventricular infusion of PEDF promotes NSC division, whereas inhibition of PEDF signaling decreases it[4]. Furthermore, injury-mediated activation of adult periventricular NSCs increases their expression of EGFR[12] and Notch signaling[13]. It may also be more reasonable for a quiescent non-EGFR expressing NSC to progress to an active EGFR-expressing NSC, initiated in part by PEDF, to generate transit-amplifying cells known to express EGFR[12]. The inability of NSCs with low levels of NICD to generate NSCs with high levels of NICD *in vitro* could simply be a cell culture limitation and their decreased capacity to generate neurospheres could be a reflection of their quiescent state. Tracing the fate of NSCs expressing high or low levels of NICD/ EGFR *in vivo* may provide some insight in the future. Because EGFR is a direct target of Notch signaling, quiescent NSCs may need shielding from excessive Notch signaling, as increasing levels of EGFR and EGF signaling have been demonstrated to inhibit neural precursor proliferation and promote astrogliogenesis[14]. In this regard, it is worth noting that Numb physically interacts with NICD to inhibit Notch signaling, but, paradoxically, it has been found to maintain the neural precursor pool during development[15].Whether Numb and PEDF signaling interact and have opposing roles in regulating adult NSC quiescence or self-renewal would also be an interesting avenue for future investigations.


1. Shen, Q. *et al. Cell Stem Cell* **3**, 289–300 (2008).
2. Tavazoie, M. *et al. Cell Stem Cell* **3**, 279–288 (2008).
3. Shen, Q. *et al. Science* **304**, 1338–1340 (2004).
4. Ramírez-Castillejo, C. *et al. Nat. Neurosci.* **9**, 331–339 (2006).
5. Nyfeler, Y. *et al. EMBO J.* **24**, 3504–3515 (2005).
6. Hitoshi, S. *et al. Genes Dev.* **16**, 846–858 (2002).
7. Andreu-Agulló, C., Morante-Redolat, J.M., Delgado, A.C. & Fariñas, I. *Nat. Neurosci.* **12**, 1514–1523 (2009).
8. Chojnacki, A.K., Mak, G.K. & Weiss, S. *Nat. Rev. Neurosci.* **10**, 153–163 (2009).
9. Reynolds, B.A. & Weiss, S. *Science* **255**, 1707–1710 (1992).
10. Hermanson, O., Jepsen, K. & Rosenfeld, M.G. *Nature* **419**, 934–939 (2002).
11. Notari, L. *et al. J. Biol. Chem.* **281**, 38022–38037 (2006).
12. Doetsch, F., Petreanu, L., Caille, I., Garcia-Verdugo, J.M. & Alvarez-Buylla, A. *Neuron* **36**, 1021–1034 (2002).
13. Givogri, M.I. *et al. Dev. Neurosci.* **28**, 81–91 (2006).
14. Burrows, R.C., Wancio, D., Levitt, P. & Lillien, L. *Neuron* **19**, 251–267 (1997).
15. Qu, Q. & Shi, Y. *J. Cell. Physiol.* **221**, 5–9 (2009).






# Hippocampal theta rhythms follow the beat of their own drum

Laura Lee Colgin & Edvard I Moser

**The firing of most hippocampal neurons is modulated by the theta rhythm, but it's not clear how and where the rhythm is generated. A study now shows that the required machinery for theta generation lies in local circuits of the hippocampus.**

The hippocampal theta rhythm is one of the largest synchronous signals in the mammalian brain. Theta rhythms are essential for linking distributed cell ensembles during key functions of the hippocampus, such as learning and spatial navigation. The search for its origins began more than 50 years ago when lesions of the medial septum were found to disrupt hippocampal theta[1]. Subsequent studies found that medial septal neurons discharged synchronously with hippocampal theta, leading researchers to suggest the medial-septum diagonal-band area as the theta pacemaker[2,3]. In this issue, Goutagny *et al.*[4] provide fresh insight into this matter by showing that theta rhythms with properties similar to those of the living animal emerge in a whole-hippocampus *in vitro* preparation without input from external sources and without the addition of any drugs that might mimic aspects of septal stimulation.

The septal pacemaker hypothesis has dominated models of theta generation since its inception. The hypothesis was challenged by reports of theta-like activity in hippocampal slices lacking input from the medial septum, but treated with agonists of acetylcholine or metabotropic glutamate receptors[5,6]. However, it was never determined whether these slice rhythms were analogous to theta in behaving animals. In some preparations, the theta oscillations appeared as intermittent bursts that partially resembled epileptic activity[7]. In others, theta was seen only when AMPA receptors were silenced[6], a condition that may never occur in the living animal. The question of whether intrahippocampal circuits are capable of theta generation has therefore remained open.

Goutagny *et al.*[4] provide evidence that drug- and septal input–free hippocampus can generate and sustain its own theta oscillation. They measured field potentials and single-neuron activity from CA1 of the isolated hippocampi, which exhibited oscillatory activity in the theta frequency range (3–10 Hz; **Fig. 1**). Depth profiles showed a near-complete phase reversal between the pyramidal cell layer and stratum radiatum, suggesting that the rhythmic pattern was generated in CA1 in a manner similar to that of the intact animal[8]. As in behaving

The authors are at the Kavli Institute for Systems Neuroscience and Centre for the Biology of Memory, Medical-Technical Research Centre, Norwegian University of Science and Technology, Trondheim, Norway.
e-mail: edvard.moser@ntnu.no

animals[9], CA1 principal cells and interneurons preferentially fired near the trough of theta oscillations in the CA1 pyramidal cell layer. The theta activity was abolished by antagonists of GABA or AMPA/kainate receptors. Theta rhythms were coherent across large parts of the longitudinal axis of CA1, but coherence between CA1 and CA3 oscillations was low. Removal of inputs from CA3 did not block the oscillations in CA1, suggesting that the two subfields have independent generators for theta activity. These results clearly suggest that theta activity is an inherent property of the hippocampal network emerging from local connectivity. External inputs, such as those from the medial septum, are not strictly required for generating or maintaining theta activity in the hippocampus.

The induction of theta rhythm in a complete hippocampal preparation provides important clues about the intrahippocampal circuit mechanisms that may sustain theta-patterned activity. In contrast with standard transverse slices, the complete preparation preserves the majority of intrahippocampal connections in the longitudinal plane, suggesting that these are more involved in theta generation than had been previously thought. The fact that theta activity was maintained in CA1 after it was disconnected from CA3 suggests that the intrinsic interneurons in CA1 are critical for generating the oscillations. Several classes of CA1 interneurons are strongly modulated by hippocampal theta activity in intact animals[10,11] and many of these interneurons extend their axons for hundreds of micrometers or even millimeters longitudinally. These longitudinal connections could be important for enabling theta rhythms in the intact hippocampi to become coherent along widespread regions along the septotemporal axis of CA1. The possible involvement of such interneurons would also explain why theta activity is difficult to induce in standard hippocampal slices.

Is there more than one hippocampal oscillator involved in theta generation? The study by Goutagny *et al.*[4] suggests that there are multiple generators and that these are distributed along the septotemporal axis of the hippocampus. When theta activity was recorded at two locations in CA1, one dorsal and one ventral, and the regions between were silenced by procaine, both regions continued to oscillate, but the ventral oscillator was slower than the dorsal oscillator by about 1 Hz. When the connections between the areas were intact, however, the faster oscillator appeared to be entraining the slower one, suggesting that the oscillators are normally coupled. The existence of multiple weakly coupled oscillators with decreasing frequencies along the septotemporal axis suggests a possible mechanism for the systematic changes in theta phase reported along the septotemporal axis in behaving animals[12] and potentially sheds light on the timing of theta-related information processing in the hippocampus.

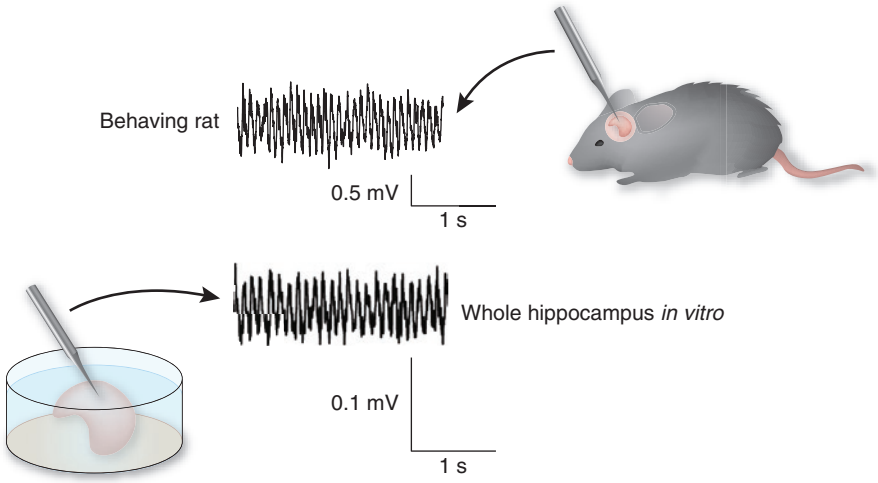


**Figure 1** The upper trace shows theta recorded from the CA1 apical dendrites of a freely moving rat (L.L.C. and E.I.M., unpublished data), whereas the lower trace shows theta waves in the whole-hippocampus preparation of Goutagny *et al.*[4] (their Fig. 1c). Note that the *in vivo* and *in vitro* patterns are almost identical in frequency, wavelength and waveform.

The presence of theta activity in the isolated hippocampal preparation does not, however, exclude a role for inputs from the medial septum. Although these inputs may not be necessary for the rhythm itself, they may, for example, be involved in synchronizing oscillators at different septotemporal levels. It is also important to be aware that there may be more than one mechanism for theta generation and that other mechanisms may require septal input. Theta oscillations in behaving animals appear in two forms[13]. One occurs during active movement and is resistant to muscarinic acetylcholine receptor antagonists. The other is associated with immobility and is abolished by muscarinic antagonists. Goutagny *et al.*[4] found that the theta rhythms were unaffected by a muscarinic antagonist, suggesting that they were analogous to movement-related theta. Thus, the septal pacemaker hypothesis may still prevail for theta that requires muscarinic receptors.

Many other interesting questions are raised by the findings of Goutagny *et al.*[4]. For example, if CA1 contains multiple theta oscillators along its longitudinal axis, are these discrete or do they form a continuous overlapping network? If they are discrete, how many are there and how are their borders defined? Are differences in oscillator frequencies related to the differences in intracellular oscillation frequencies for pyramidal cells at different septotemporal locations[14]? Moreover, what are the components of the CA1 circuit responsible for theta generation? Which types of interneurons are involved and what are their relative contributions? Do these interneurons correspond to the classes of theta-related interneurons that have been defined *in vivo*[11]? And finally, can the whole-hippocampus preparation switch from theta activity to other hippocampal network states or are external inputs needed for such transitions? The introduction of spontaneously occurring, stable theta rhythms in an *in vitro* preparation by Goutagny *et al.*[4] paves the way for such analyses in the years to come.

1. Green, J.D. & Arduini, A.A. *J. Neurophysiol.* **17**, 533–557 (1954).
2. Petsche, H., Stumpf, C. & Gogolak, G. *Electroencephalogr. Clin. Neurophysiol.* **14**, 202–211 (1962).
3. Stewart, M. & Fox, S.E. *Trends Neurosci.* **13**, 163–168 (1990).
4. Goutagny, R., Jackson, J. & Williams, S. *Nat. Neurosci.* **12**, 1491–1493 (2009).
5. Konopacki, J., Bland, B.H. & Roth, S.H. *Brain Res.* **451**, 33–42 (1988).
6. Gillies, M.J. *et al. J. Physiol. (Lond.)* **543**, 779–793 (2002).
7. Williams, J.H. & Kauer, J.A. *J. Neurophysiol.* **78**, 2631–2640 (1997).
8. Bland, B.H. *Prog. Neurobiol.* **26**, 1–54 (1986).
9. Csicsvari, J., Hirase, H., Czurko, A., Mamiya, A. & Buzsaki, G. *J. Neurosci.* **19**, 274–287 (1999).
10. Buzsáki, G. *Neuron* **33**, 325–340 (2002).
11. Somogyi, P. & Klausberger, T. *J. Physiol. (Lond.)* **562**, 9–26 (2005).
12. Lubenov, E.V. & Siapas, A.G. *Nature* **459**, 534–539 (2009).
13. Kramis, R., Vanderwolf, C.H. & Bland, B.H. *Exp. Neurol.* **49**, 58–85 (1975).
14. Maurer, A.P., Vanrhoads, S.R., Sutherland, G.R., Lipa, P. & McNaughton, B.L. *Hippocampus* **15**, 841–852 (2005).

nature neuroscience

# Self-generated theta oscillations in the hippocampus

Romain Goutagny[1,2], Jesse Jackson[1,2] & Sylvain Williams[1]

**Hippocampal theta rhythm is crucial for spatial memory and is thought to be generated by extrinsic inputs. In contrast, using a complete rat hippocampus *in vitro*, we found several intrinsic, atropine-resistant theta generators in CA1. These oscillators were organized along the septotemporal axis and arose independently from CA3. Our results suggest that CA1 theta rhythm can emerge from the coupling of multiple autonomous hippocampal theta oscillators.**

Episodic and spatial memory, the ability to recollect past events and locations, requires the sequential binding of cell assemblies over a temporal metric provided by theta-frequency oscillations[1]. Traditional models of hippocampal theta rhythm generation emphasize the necessity of a synchronizing extrinsic rhythm generator that is thought to arise from the medial septum. However, theoretical studies[2,3] suggest that the hippocampus may possess the minimal circuitry required for theta periodicity. The lack of experimental evidence to support this concept may be a result of the fact that the hippocampal slice preparation is not adequate for the study of complete intrinsic hippocampal network properties[4]. To circumvent this issue, we performed extracellular field recording in the intact isolated hippocampus *in vitro* (from rats postnatal day 15–28; **Fig. 1a**, **Supplementary Methods** and **Supplementary Fig. 1**).

After 10–50 min in the recording chamber (**Fig. 1b–d**), CA1 area exhibited self-sustained, continuous theta activity (5.1 ± 0.2 Hz, range = 3–10 Hz, mean theta waveform amplitude = 0.124 ± 0.007 mV, range = 0.033–0.331 mV, $n$ = 62) at a similar frequency as has been seen in *in vivo* recordings[5–7] and that lasted up to 120 min (**Supplementary Fig. 2**). The wave-shape of the theta oscillation varied according to frequency and maintained a symmetrical near-sinusoidal shape similar to *in vivo* theta rhythm (**Supplementary Figs. 3** and **4**). Using identical experimental conditions, we found that theta was not generated in transverse or horizontal hippocampal slices (500 µm, $n$ = 5; **Supplementary Fig. 5**). The depth profile of the recorded theta activity demonstrated a near-complete phase shift from stratum oriens to stratum radiatum (164 ± 11°, range = 116–208°; **Supplementary Fig. 6**) and current source density measurements revealed the presence of a single sink-source alternation between the pyramidal cell layer (with high multiunit activity) and stratum radiatum (**Fig. 1d**). This hippocampal theta was observed using normal artificial cerebrospinal fluid, but was reduced or abolished by increasing either excitatory or inhibitory tone (**Supplementary Figs. 7** and **8**).

To assess the neurotransmitters involved in this oscillation, we bath-applied different antagonists for cholinergic, glutamatergic and GABAergic neurotransmission (**Supplementary Fig. 9** and

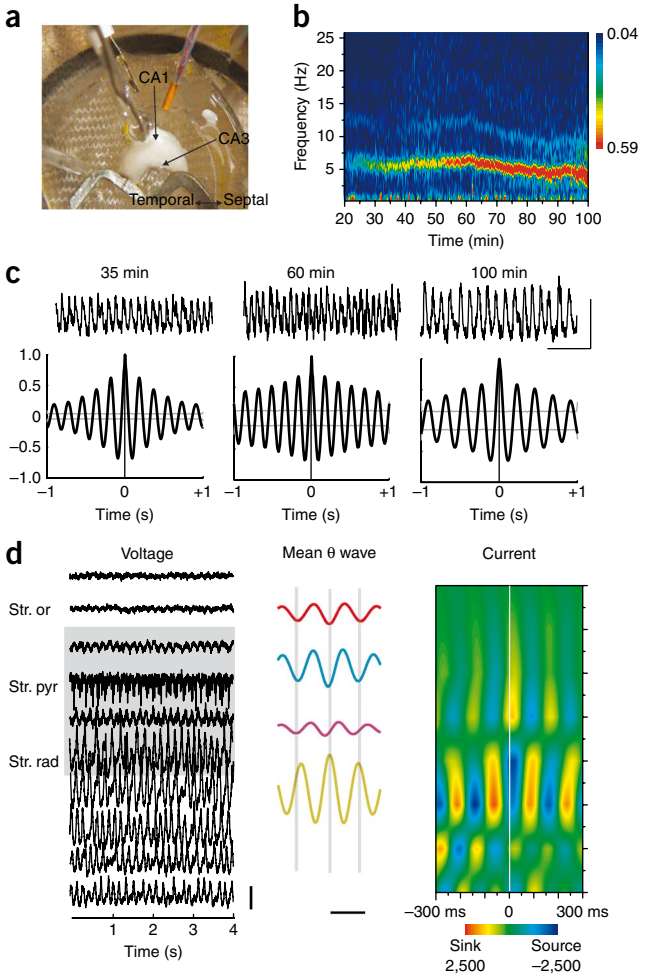


**Figure 1** Descriptive properties of theta rhythm in the isolated hippocampus. (**a**) A photograph of the complete hippocampal preparation. (**b**) Spectrogram showing the emergence of continuous CA1 theta oscillations in the isolated hippocampus *in vitro*. (**c**) Representative raw data and corresponding autocorrelations from the same experiment shown in **b** at the times indicated. Scale bars represent 0.1 mV and 1 s. (**d**) Left, raw data from 75-µm increments through the distal CA1 region in the middle hippocampus. Middle, averaged filtered traces from four sequential depths demonstrating the rapid complete phase reversal over 150 µm. Right, current source density of the averaged theta wave (triggered from stratum radiatum), demonstrating a single sink/source dipole. Scale bars represent 0.1 mV and 200 ms.

[1]Douglas Mental Health University Institute, McGill University, Department of Psychiatry, Montréal, Québec, Canada. [2]These authors contributed equally to this work. Correspondence should be addressed to S.W. (sylvain.williams@douglas.mcgill.ca).

Received 8 June; accepted 29 September; published online 1 November 2009; doi:10.1038/nn.2440

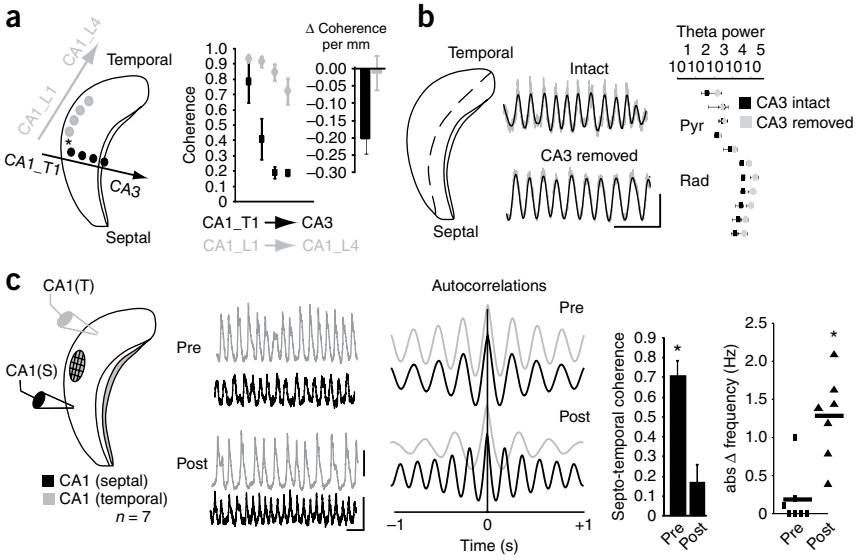


**Figure 2** Topography of the spontaneous theta oscillation recorded in CA1. (**a**) Recording electrodes were moved (1-mm intervals) along both transverse and longitudinal axes, as shown by the location of black and gray dots. The coherence was measured in both axes and the position of the point is indicated by the arrow below the plot. The change in coherence per mm dropped at a rate of –0.2 ± 0.04 per mm in the transverse plane, whereas it dropped in the longitudinal axis by only 0.01 ± 0.05 per mm ($t_3$ = 3.06, $P$ = 0.055). CA1_L1, longitudinal 1; CA1_L4, longitudinal 4; CA1_T1, transverse 1. (**b**) Removal of CA3 did not prevent the emergence of theta activity. Example raw data (gray) and theta-filtered (3–12 Hz) data (black) of activity recorded in two separate preparations with and without CA3. Right, theta power versus depth for intact ($n$ = 6) and CA3-removed ($n$ = 4) conditions. (**c**) The experimental procedure used to identify independent intrahippocampal theta oscillators. Procaine (gray ellipse with hatched lines) was infused between two recording electrodes. Representative raw data (0.1–500 Hz) recorded from the septal and temporal poles of the hippocampus before (top) and 2 min after procaine infusion (bottom) between the two hippocampal sites, unmasking the presence of two separate frequencies in the two recordings, as shown in the autocorrelations. The maximal septo-temporal theta coherence between the two recording electrodes decreased following procaine infusion as a result of the two regions oscillating at two distinct frequencies (mean absolute difference = 1.3 Hz, far right). Scale bars in **b** and **c** represent 500 ms and 0.1 mV.



**Supplementary Table 1**). Given that two types of hippocampal theta can be identified *in vivo* on the basis of sensitivity to muscarinic receptor blockers[8], we first applied atropine sulfate (10 μM, 10 min, $n$ = 9) and observed no change in either the power ($F_{2,24}$ = 3.07, $P$ = 0.17) or frequency ($F_{2,24}$ = 2.27, $P$ = 0.13) of the theta oscillations. The CA1 theta oscillations were only abolished by the application of the AMPA/kainate receptor antagonist 6,7-dinitroquinoxaline-2,3-dione (DNQX, 10 μM, 10 min, $n$ = 6, $F_{2,15}$ = 54.75, $P$ < 0.001; **Supplementary Fig. 9**) or the $GABA_A$ receptor antagonist bicuculline (5 μM, 2 min, $n$ = 6, $F_{2,12}$ = 130.3, $P$ < 0.0001; **Supplementary Fig. 9**). Taken together, these results indicate that the isolated hippocampus can generate self-sustained theta oscillations without cholinergic activation or afferent inputs.

We then examined the topography of this theta oscillation by measuring theta-band coherence along both the longitudinal (septotemporal) and transverse (CA3–CA1) axes using the distal CA1 as a reference. Theta-band coherence remained high along the longitudinal axis, but exhibited significant decreases over the transverse axis ($F_{3,12}$ = 8.04, $P$ = 0.003), with the lowest coherence in CA3 (**Fig. 2a**), indicating that this intrinsic theta oscillation is preferentially organized along the longitudinal axis of CA1. These data suggest that the CA1 oscillations arise independent of CA3.

To definitively test this hypothesis, we surgically removed CA3 during the dissection (**Supplementary Fig. 10**). The removal of CA3 did not impair the ability of the CA1 region to generate self-sustained theta rhythm (**Fig. 2b**). No significant change in theta frequency ($n$ = 8, 5.0 ± 0.4 Hz, $P$ > 0.05) or in the phase shift was observed in the absence of CA3 ($n$ = 4, 186 ± 15°, $P$ > 0.05). Therefore, CA1 theta oscillations can arise independent of CA3 inputs in the isolated hippocampus *in vitro*. These results indicate that the CA1 area of the hippocampus contains the sufficient circuitry to spontaneously and independently generate theta oscillations *in vitro*. As a result, the dissociable mechanisms of spatial encoding between CA1 and CA3 (refs. 1,9) may be explained by the presence of separate intrinsic theta oscillators in each region.

We then tested whether local inactivation of part of the CA1 region would uncouple theta oscillations recorded 4–5 mm apart in the septotemporal direction. Blockade of synaptic transmission (20% procaine hydrochloride, vol/vol, 0.1–0.3 μL) between two electrodes positioned at the septal and temporal poles reduced the peak coherence (0.71 ± 0.09 pre, 0.16 ± 0.10 post procaine, $t_6$ = 5.22, $P$ = 0.002) of theta (**Fig. 2c**) without altering hippocampal theta power (**Supplementary Fig. 11**). This uncoupling was a result of the emergence of two distinct oscillators with different frequencies (the absolute difference in peak frequency = 0.2 ± 0.1 Hz pre versus 1.3 ± 0.2 Hz post, $t_6$ = 3.63, $P$ = 0.01; **Fig. 2c**). Moreover, the faster oscillator following procaine showed a slight lead in the pre-procaine condition (49 ± 26 ms), suggesting that this oscillator was entraining the slower oscillator. Similar infusions of procaine in CA3 did not alter the properties of the CA1 rhythm (**Supplementary Fig. 11**). These results indicate that multiple theta oscillators with different frequencies coexist along the longitudinal axis of CA1 (**Supplementary Fig. 12**) and that a collective population rhythm can emerge via phase entrainment of theta oscillators of different inherent frequencies. This concept is consistent with a recent study suggesting that *in vivo* hippocampal theta wave propagation arises from a network of weakly coupled theta oscillators[10].

At the cellular level, extracellular recordings of putative principle cells and interneurons ($n$ = 29) both demonstrated significant phase locking to the extracellular field potential (159 ± 11°, $P$ < 0.01 using the Rayleigh test for uniformity, theta peak recorded from radiatum is 180°; **Supplementary Fig. 13**), indicating that theta oscillations in CA1 entrain pyramidal cells and interneurons. To further investigate how these cells were synaptically entrained during theta-band network activity, we performed whole-cell recordings of pyramidal cells ($n$ = 5) and interneurons ($n$ = 12; **Fig. 3**).

At resting membrane potential, the principle cells did not fire action potentials, but instead had rhythmic synaptic potentials ($n$ = 4 cells were phase-locked to the extracellular oscillation). Principle cells were driven at rest by prominent phasic inhibitory postsynaptic potentials (IPSPs, mean amplitude of −3.8 mV, **Fig. 3a**,**c**) and clearly showed rebound spiking following the IPSP when depolarized (mean phase of 120°; **Fig. 3a**,**c**) on a similar (although slightly earlier) phase as pyramidal cells *in vivo*[5,11,12]. Two pyramidal cells

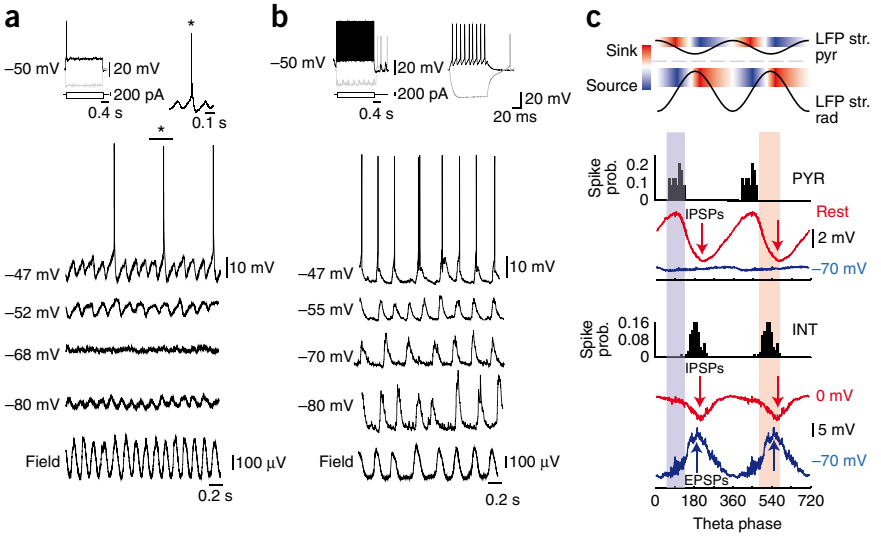


**Figure 3** Synaptic activity during the spontaneous theta oscillations. (**a**) Synaptic activity recorded in a pyramidal cell during theta oscillations. This cell was driven by prominent IPSPs at rest, but the IPSPs were at equilibrium near –68 mV and reversed in polarity with further membrane hyperpolarization. (**b**) Synaptic activity of an example fast-firing interneuron during spontaneous theta oscillation. This cell was driven by EPSPs at rest. (**c**) A potential mechanism for the generation of hippocampal theta on the basis of our data. Top, two cycles of extracellular theta are shown and the corresponding sink-source alternations are shown as in **Figure 1**. Below, data from a principle cell (PYR) and an interneuron (INT) are shown, with the spiking and synaptic activity thought to underlie the sink source alternation. The large number of sparsely firing principle cells fired on the falling phase of theta recorded from stratum pyramidale and corresponding to the sink in this layer. This elicited EPSPs and spiking in interneurons, which subsequently feedback onto principle cells. Thus, interneuron spiking was maintained by the sparsely firing pyramidal cell network. The interneuron spike elicited IPSPs in a large principle-cell population, thus resetting the membrane potential to a common phase and corresponding to the source in stratum pyramidale and passive sink in radiatum. In addition, synaptically connected interneurons elicited IPSPs shortly after interneuron spiking (shown in red). LFP, local field potential.

were driven by small-amplitude excitatory postsynaptic potentials (EPSPs) at rest (mean of 1.4 mV), as well as phase-locked IPSPs when the cells are depolarized at 0 mV (mean amplitude of −2.2 mV). These results indicate that CA1 pyramidal cells are paced by interneurons during spontaneous theta oscillations and that a subset of these cells also receives excitatory inputs from other principle cells[13].

Interneurons exhibited prominent phasic EPSPs at rest that correlated to the theta oscillation (mean amplitude of 5.4 ± 1.1 mV, $n = 9$ of 12; **Fig. 3b**) and fired action potentials (mean frequency of 3.2 ± 0.7 Hz, $n = 7$) that were phase-locked to the extracellular theta oscillation (mean phase of 195 ± 4°; **Fig. 3b**,**c**). In all of the interneurons tested ($n = 3$), it was also possible to identify an inhibitory driving component that was phase-locked to the local field potentials when the cells were held at 0 mV (mean amplitude of −4.1 ± 0.9 mV). These results indicate that CA1 interneurons are mainly driven by local principle cells during spontaneous theta oscillation and that they also received inhibitory inputs. Therefore, similar to many other biological network oscillators[14], a feedback loop between principle cells and inhibitory interneurons[15] appears to be necessary and sufficient for the emergence of this *in vitro* theta rhythm (**Fig. 3c**).

Our results show that the CA1 area of the hippocampus contains the sufficient intrinsic circuitry to spontaneously generate theta oscillations, indicating that the CA1 region can undergo a previously unappreciated form of long range theta synchronization without a precise clocking input (see **Supplementary Discussion**).

*Note: Supplementary information is available on the Nature Neuroscience website.*

**ACKNOWLEDGMENTS**

We thank M. Danik, G. Ducharme, C.K. Young, C.T. Dickson and G. Buzsaki for their comments on the manuscript. This work was supported by the Canadian Institute of Health Research, the Natural Sciences and Engineering Research Council of Canada and the Fonds de la Recherche en Santé du Québec. R.G. was supported by the Conrad F. Harrington post-doctoral fellowship from the McGill Faculty of Medicine. J.J. received a Canadian Graduate Scholarship from the Natural Sciences and Engineering Research Council of Canada and S.W. is a Fonds de la recherche en santé du Québec chercheur boursier "senior."

**AUTHOR CONTRIBUTIONS**

R.G., J.J. and S.W. designed the experiments, R.G. and J.J. performed the experiments and analyzed the data, and R.G., J.J. and S.W. wrote the paper.

Published online at http://www.nature.com/natureneuroscience/.
Reprints and permissions information is available online at http://www.nature.com/reprintsandpermissions/.

1. Hasselmo, M.E. *Hippocampus* **15**, 936–949 (2005).
2. Traub, R.D., Miles, R. & Wong, R.K. *Science* **243**, 1319–1325 (1989).
3. White, J.A., Banks, M.I., Pearce, R.A. & Kopell, N.J. *Proc. Natl. Acad. Sci. USA* **97**, 8128–8133 (2000).
4. Amaral, D.G. & Witter, M.P. *Neuroscience* **31**, 571–591 (1989).
5. Bland, B.H. *Prog. Neurobiol.* **26**, 1–54 (1986).
6. Buzsáki, G. *Neuron* **33**, 325–340 (2002).
7. Vanderwolf, C.H. *Electroencephalogr. Clin. Neurophysiol.* **26**, 407–418 (1969).
8. Kramis, R., Vanderwolf, C.H. & Bland, B.H. *Exp. Neurol.* **49**, 58–85 (1975).
9. Leutgeb, S., Leutgeb, J.K., Treves, A., Moser, M.B. & Moser, E.I. *Science* **305**, 1295–1298 (2004).
10. Lubenov, E.V. & Siapas, A.G. *Nature* **459**, 534–549 (2009).
11. Fox, S.E., Wolfson, S. & Ranck, J.B. Jr. *Exp. Brain Res.* **62**, 495–508 (1986).
12. Csicsvari, J., Hirase, H., Czurko, A., Mamiya, A. & Buzsaki, G. *J. Neurosci.* **19**, 274–287 (1999).
13. Crépel, V., Khazipov, R. & Ben-Ari, Y. *J. Neurophysiol.* **77**, 2071–2082 (1997).
14. Andersen, P. & Eccles, J. *Nature* **196**, 645–647 (1962).
15. Cobb, S.R., Buhl, E.H., Halasy, K., Paulsen, O. & Somogyi, P. *Nature* **378**, 75–78 (1995).

**Self-generated theta oscillations in the hippocampus**

Romain Goutagny, Jesse Jackson and Sylvain Williams

Supplementary information: - Supplementary figures 1 to 13

- Supplementary table 1

- Methods

- Supplementary discussion



Nature Neuroscience: doi:10.1038/nn.2440

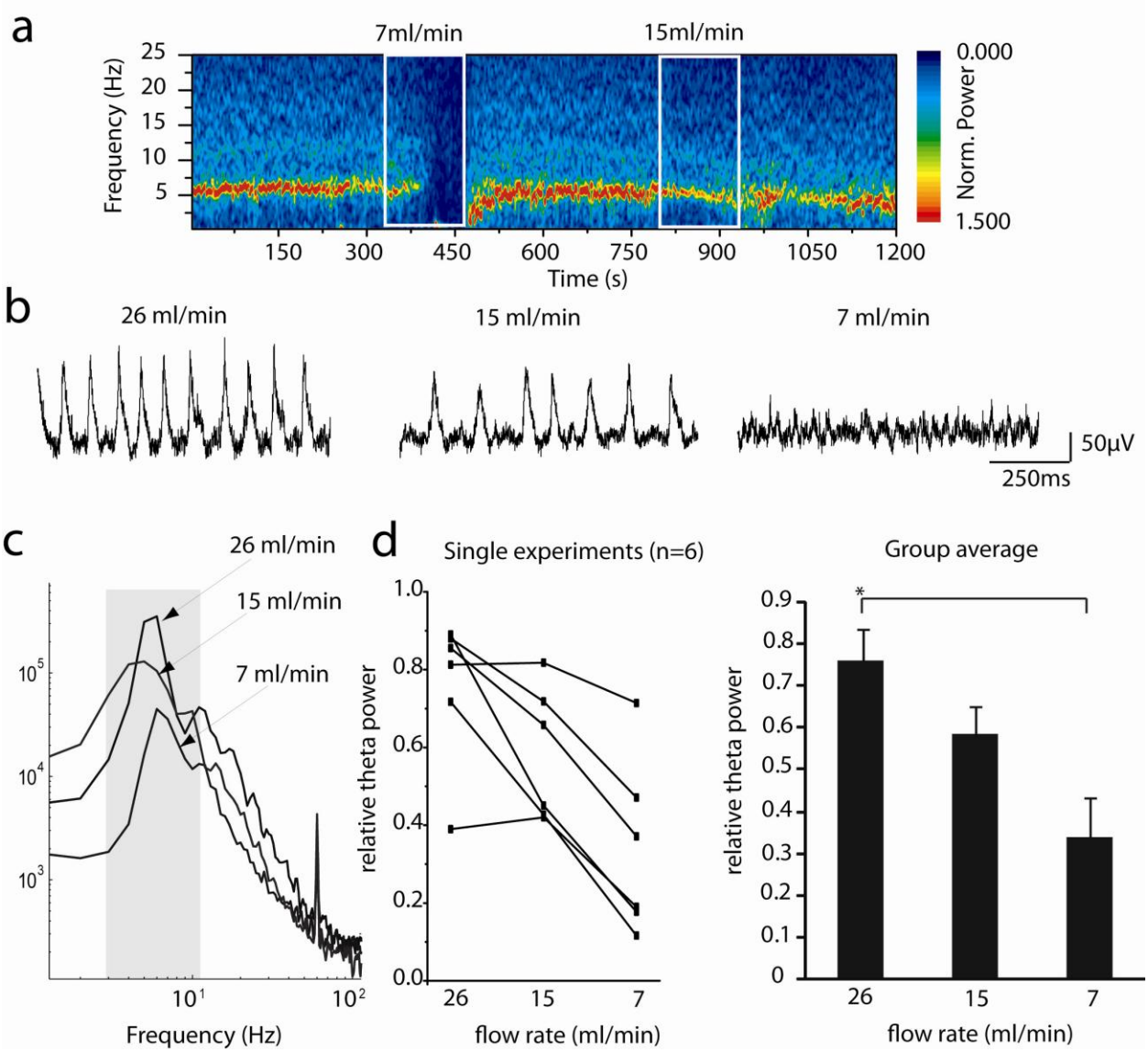


**Supplementary Figure 1:** Theta power was measured with three different aCSF flow rates. **a:** spectrogram of a representative experiment with the manipulation of aCSF flow rate during the periods indicated by the white box. After the oscillation became stable, the flow rate was decreased from 26ml/min to either 15 or 7ml/min for brief 3-5minute periods. **b:** example traces of oscillatory activity recorded from CA1 stratum radiatum during the three flow rates. **c:** an example power spectrum for activity during each flow rate. **d:** single experiments (left) and group averages (right) for theta power during each flow rate. The theta power was measured during the last 30s of these periods of reduced flow. Reducing the flow to 7ml/min reduced theta power ($p=0.006$) relative to 26ml/min. There was no statistical difference between 26 and 15 ml/min or 15 and 7 ml/min, although a trend was noted in the single experiments. No difference in frequency was noted between these conditions.



Nature Neuroscience: doi:10.1038/nn.2440

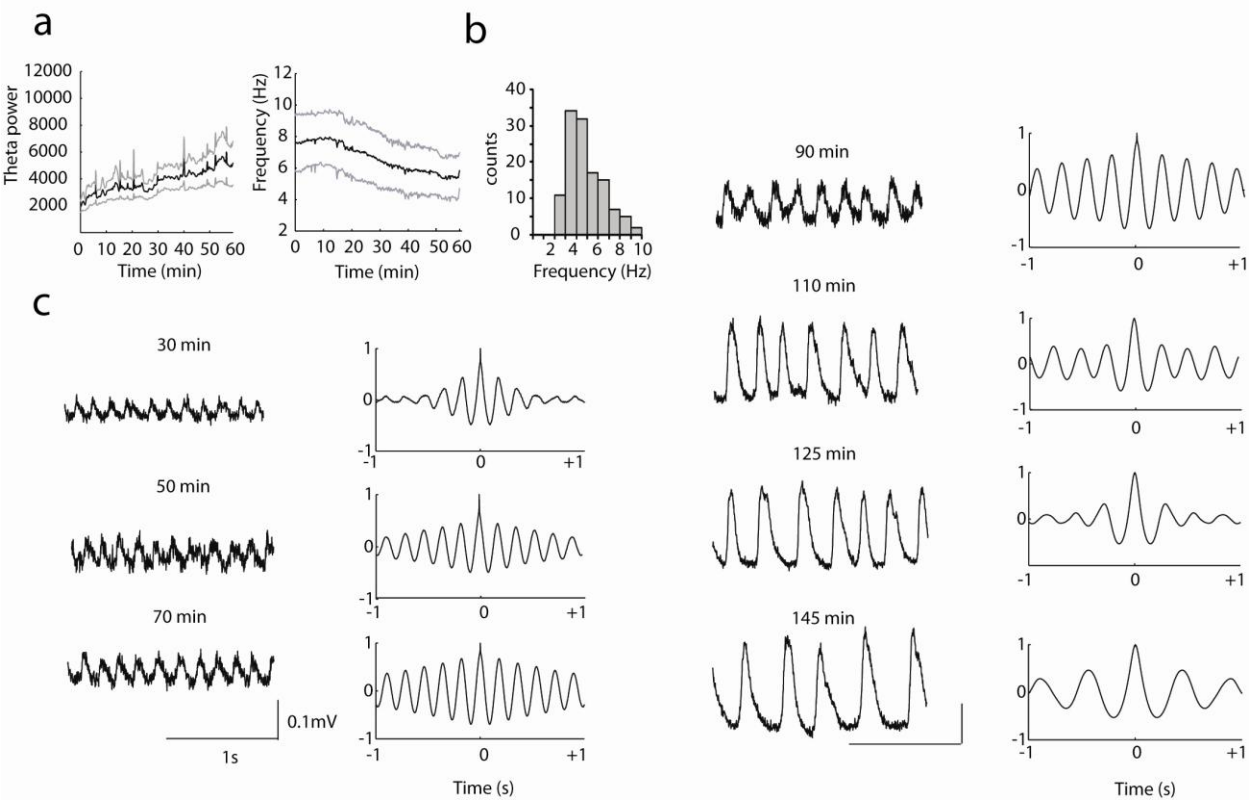


**Supplementary Figure 2: a:** Progression of theta frequency and power across time. On average, hippocampal theta frequency in this preparation decreased over time at a rate of 1Hz per 30 minutes (black line, mean; grey line, standard error). Theta power maintained an inverse correlation with theta frequency. **b:** Histogram of the peak frequency achieved in the experiments. Most hippocampal isolates oscillated at between 4-8 Hz with few cases of 3 or 10Hz. **c:** the progression of theta across time in one experiment. Theta is relatively constant for 60-90minutes but the reduction of frequency often lead to lower network oscillations at 2Hz (>2 hours in the bath) which likely arises from separate network mechanisms and thus experiments were not performed on preparations when the frequency was below the theta range. Time scale on the right is the same as the left.



Nature Neuroscience: doi:10.1038/nn.2440

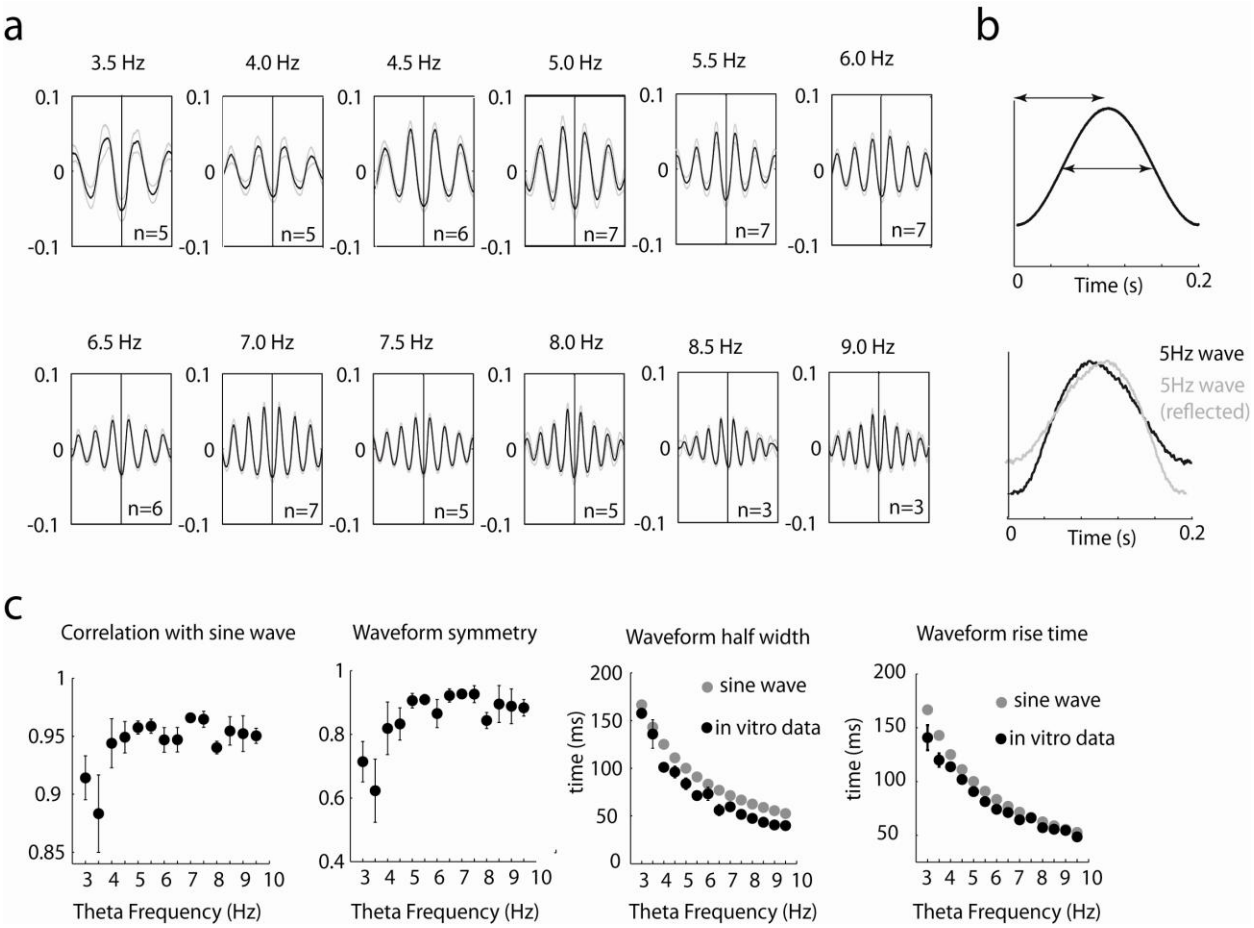


**Supplementary Figure 3:** Sinusoidal appearance of hippocampal theta oscillations *in vitro* at various frequencies (from 3.5 to 9 Hz in 0.5 Hz increments). **a:** *In vitro* hippocampal theta oscillation triggered average for each theta frequency ranging from 3.5 to 9 Hz in 0.5 Hz increments. Mean (black line) and standard error (grey lines) from data collected for 2 minutes of continuous activity at the frequency indicated above. The trough of the filtered theta oscillations (3-12 Hz) was used as the trigger, and then raw data (0.1-500 Hz) was collected from -0.5 s to +0.5 s from theta trough, therefore each inset is 1s in length. **b:** a 5Hz sine wave with arrows demonstrating how the properties of wave shape were measured. Half width was taken as the width (in ms) of the mean theta wave at half of the trough-peak amplitude. Rise time was the length of time (in ms) to the wave peak from wave trough. Shown below are the mean 5Hz single waveform and the 5 Hz waveform reflected in time. The reflected waveform was used to measure waveform symmetry by calculating the correlation between the original and reflected waveform. **c:** quantification of waveform properties across frequency using the correlation with a pure sine wave of the same frequency, waveform symmetry, half width, and rise time. The lower theta frequencies (3-3.5 Hz) have the most asymmetrical waveforms due to fast rise times. Most experiments in this study had frequencies ranging from 4-8 Hz which corresponds to the most sinusoidal waveforms.



Nature Neuroscience: doi:10.1038/nn.2440

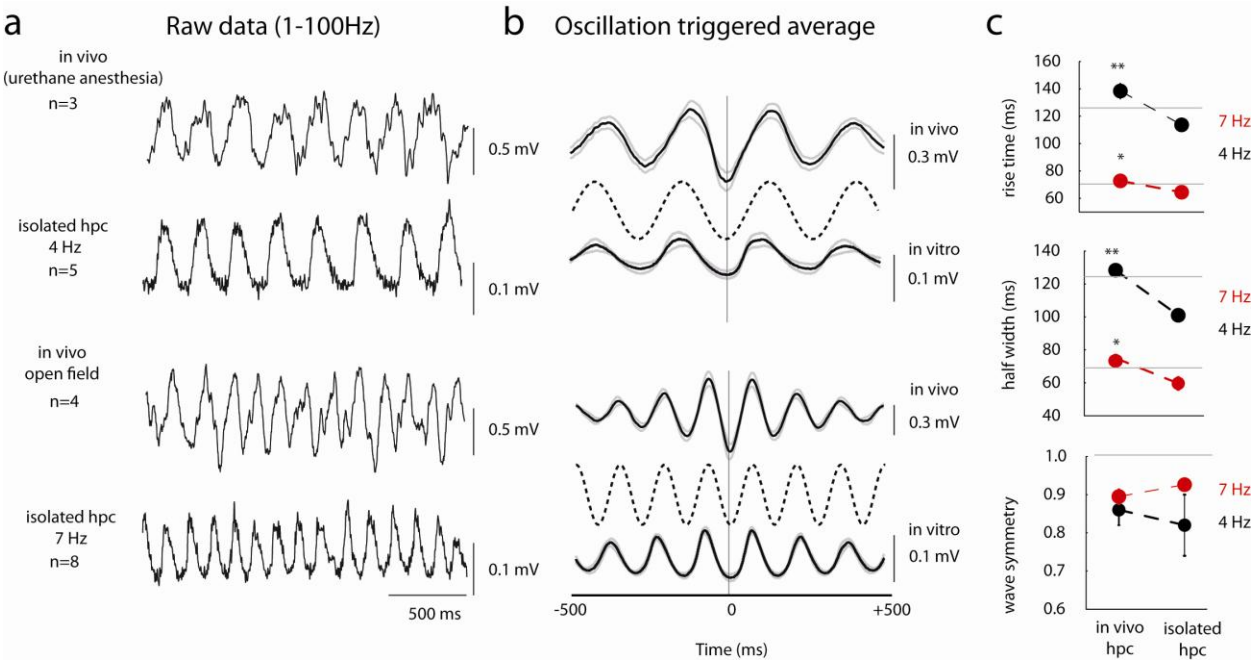


**Supplementary Figure 4:** A comparison of spontaneous *in vitro* theta oscillation wave-shape in the present study and *in vivo* theta oscillations. **a:** Data from urethane anesthetized rats which typically produce lower frequencies (3-5 Hz) were compared to *in vitro* data and matched for frequency at 4Hz. *In vivo* data from an animal exploring an open field maze was compared to *in vitro* data matched for frequency (resolution 0.25 Hz). **b:** oscillation triggered average of theta activity (triggered on theta trough), mean (black) and standard error (grey) are shown. Also shown are sine waves (dashed lines) of 3.5 Hz (top) and 7 Hz (bottom) for comparison. **c:** quantification of theta rise time, half width, and waveform symmetry for *in vivo* and *in vitro* data. The 4 Hz and 7 Hz *in vitro* data had a shorter rise time and half width than *in vivo* data at the same frequency. However, waveform symmetry was not different between *in vivo* and *in vitro*. Therefore, it seems as though both *in vivo* and *in vitro* data have a slight saw-tooth shape, yet in different directions with *in vivo* waves rising slower and decaying fast whereas *in vitro* waves rise fast and decay slow. The gray lines indicate the values for pure sine waves of 4 and 7 Hz. It was also noted that the waveforms from freely moving animals were more variable due to rapid shifting between frequencies. The *in vivo* data used here were from [1, 2]. * <0.05, ** <0.01.



Nature Neuroscience: doi:10.1038/nn.2440

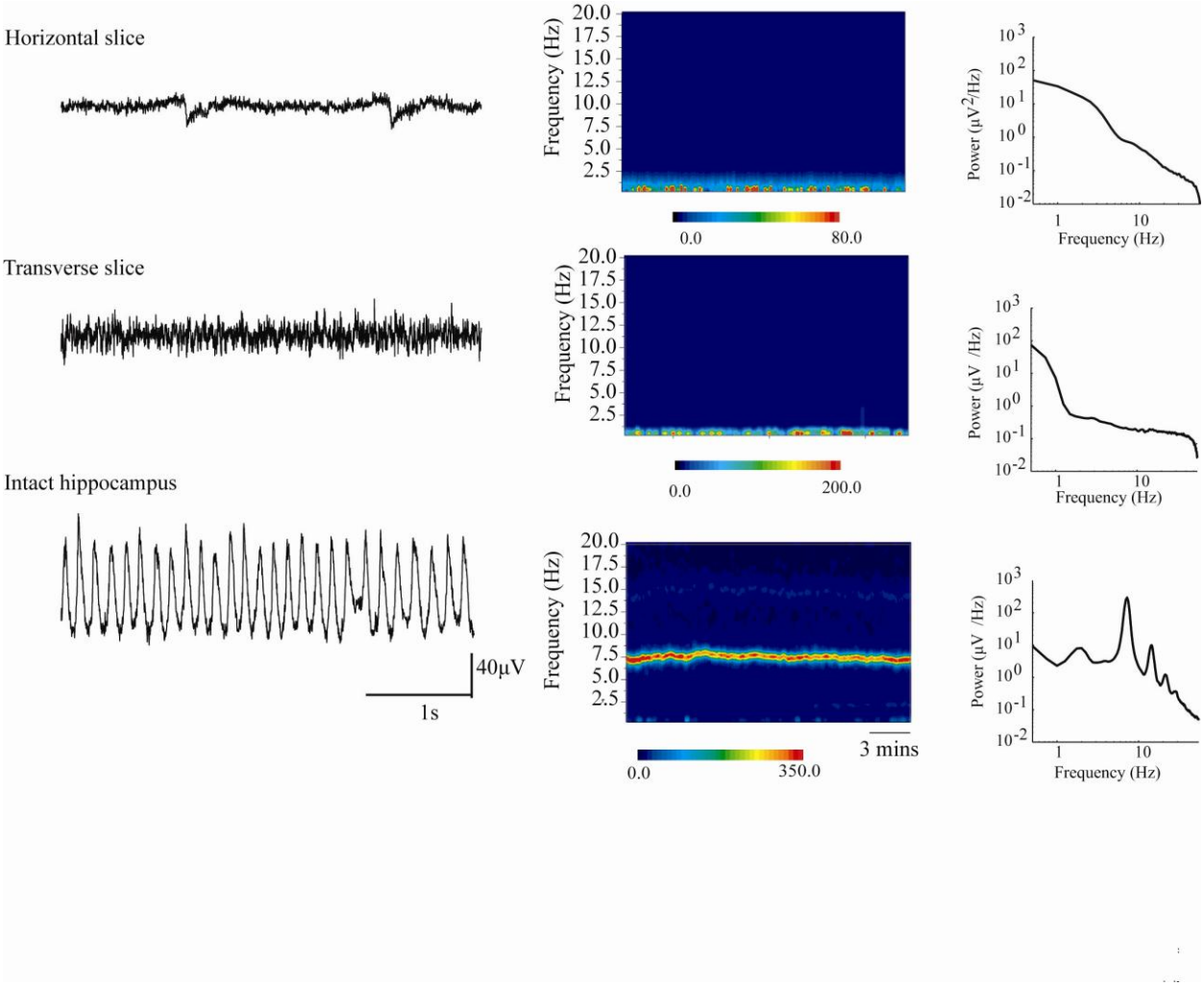


**Supplementary Figure 5:** Hippocampal theta was not observed in slices (500 µm thick) recorded under identical recording conditions as in the intact hippocampus. Left: Four seconds of raw data are shown 1 hour following placement of the tissue into the submerged recording chamber in all three experiments. Middle: Spectrograms showing 10 minutes of activity in all three conditions demonstrating the lack of theta oscillations in slices. Note the stationary nature of the theta recorded in the whole hippocampus. Right: Mean power spectrums from all three experiments taken from the 10 minutes shown in the spectrograms.



Nature Neuroscience: doi:10.1038/nn.2440

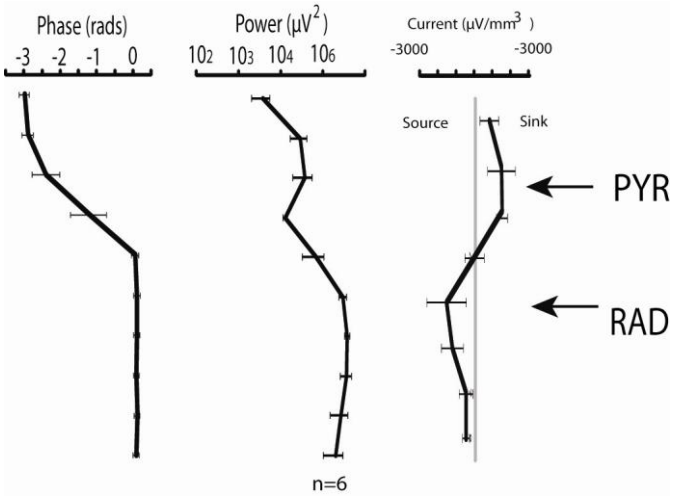


**Supplementary Figure 6:** Quantification of the theta power, phase and current recorded at 75μm increments through the distal CA1 region starting from the hippocampal surface in stratum oriens.



Nature Neuroscience: doi:10.1038/nn.2440

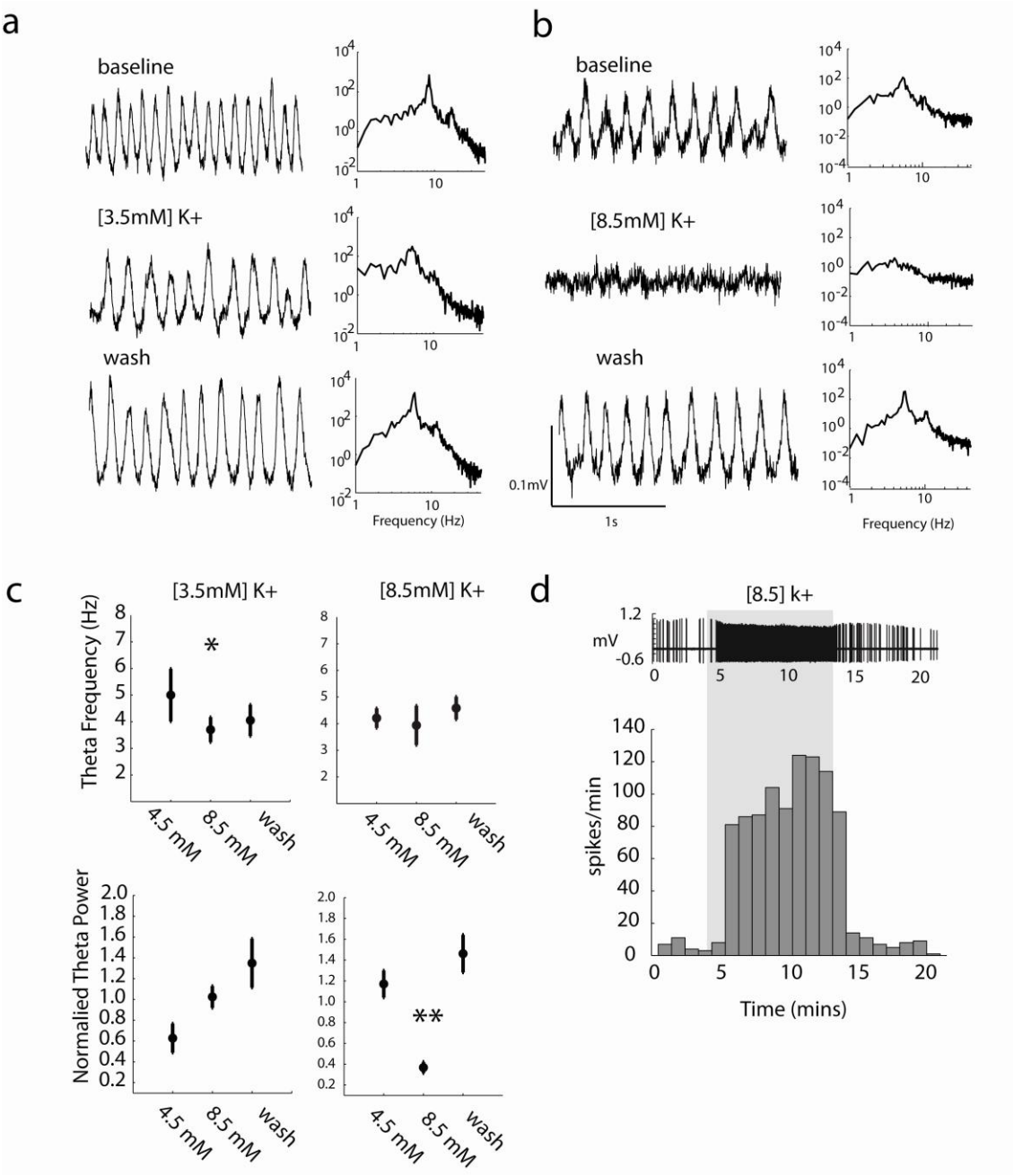


**Supplementary Figure 7:** *In vitro* theta oscillations in the isolated hippocampus are present with lower levels of extracellular potassium concentration (3.5-4.5 mM), but are reduced or abolished by increasing excitability with high potassium levels (8.5 mM). **a:** Reducing extracellular potassium from 4.5 mM to 3.5 mM (10 minutes) reduced the frequency but not the power of theta oscillations. **b:** 8.5 mM potassium (5-10 minutes) reduced theta power without an effect on frequency. **c:** group data for all experiments, * $p < 0.05$, ** $p < 0.001$. The effect of



Nature Neuroscience: doi:10.1038/nn.2440

frequency was not significant using raw values but when frequency was normalized to the experimental mean, there was a significant reduction. In some experiments the frequency of theta increases briefly with 8.5 mM potassium but it was not observed in all cases. Consistent theta activity was also generated using 3.8 mM potassium in the ACSF for the entire duration of the experiment. The ideal ACSF potassium concentration is estimated to be between 4-4.5 mM consistent to what is thought to be present in the hippocampus *in vivo*[3]. **d:** Increase in spiking activity in an example principle cell with the application of high potassium for the duration indicated by the gray box, demonstrating an increase in cell excitability. Raw extracellular data is shown on the top and a raster of spikes/minute are shown below.



Nature Neuroscience: doi:10.1038/nn.2440

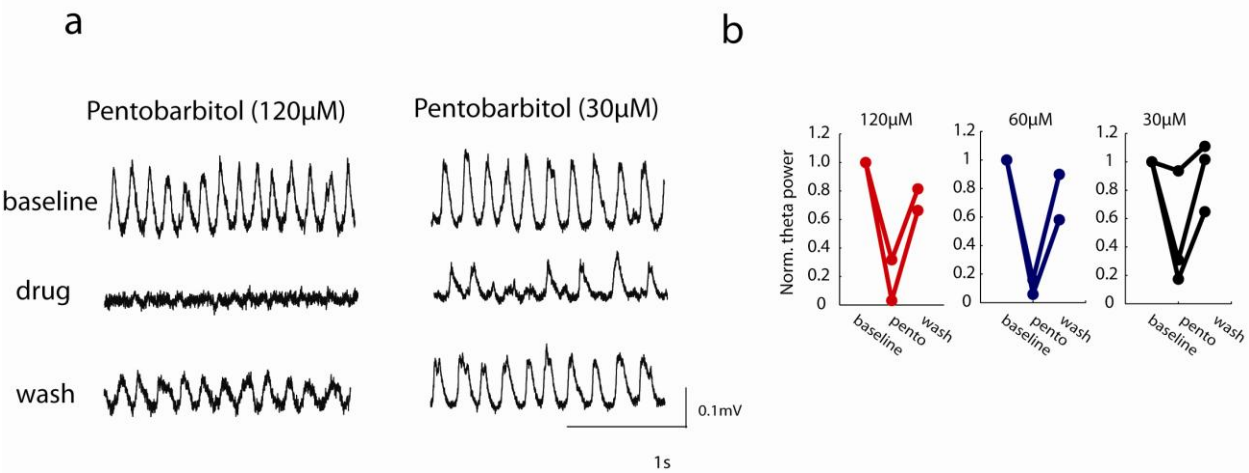


**Supplementary Figure 8:** Increasing GABAergic receptor response via the barbiturate pentobarbital abolishes theta in a dose dependent manner (30-120 µM). **a:** raw data from baseline, pentobarbital, and during washout for two different concentrations. **b:** quantification of theta power from each condition. When 120 µM and 60 µM experiments were combined ($n = 4$), there was a significant reduction in theta power relative to baseline and washout ($p < 0.05$).



Nature Neuroscience: doi:10.1038/nn.2440

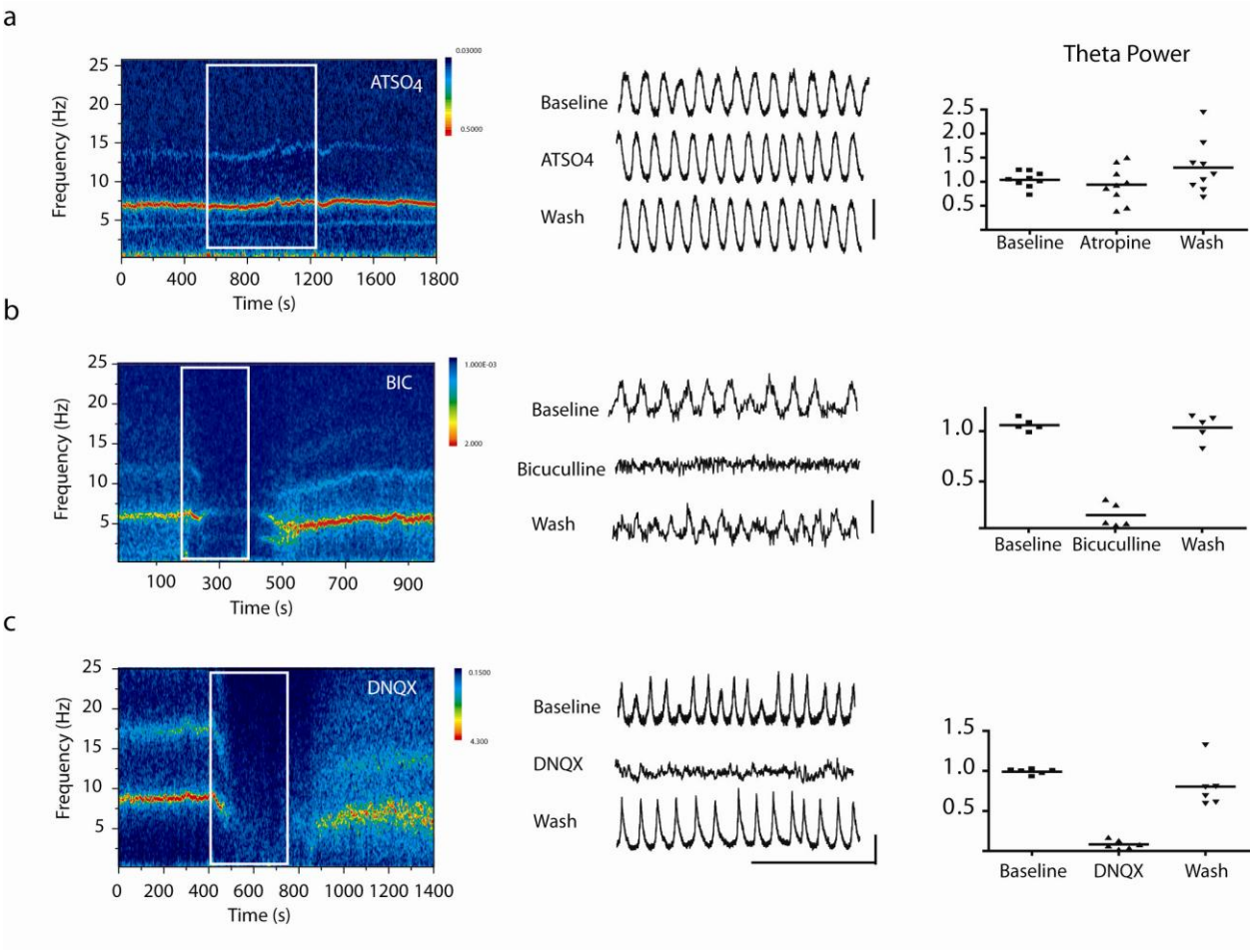


**Supplementary Figure 9:** Representative examples of pharmacological experiments where **a:** atropine sulfate (50 µM), **b:** bicuculline (5 µM), and **c:** DNQX (10 µM) were applied to the tissue for the duration indicated with the white box. Spectrograms are shown on the left. Raw data 0.1-500 Hz are shown in the middle, scale bars are 0.1 mV and 1 s. On the left is the group data showing the effect of each drug on theta power. Atropine does not abolish theta oscillations, while DNQX and bicuculline do.



Nature Neuroscience: doi:10.1038/nn.2440

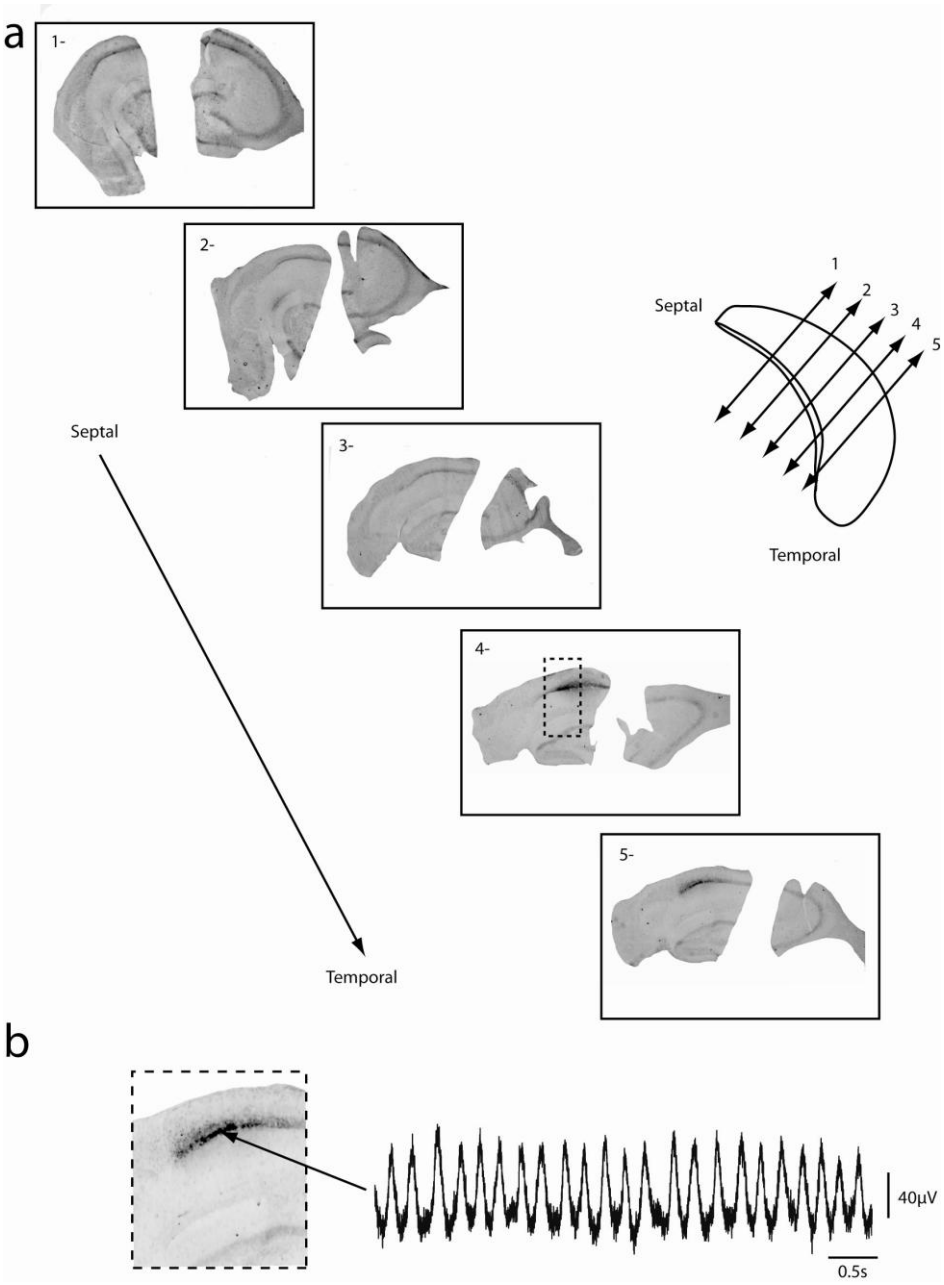


**Supplementary Figure 10:** Removal of CA3 does not abolish theta oscillations in CA1. **a:** 5 tangential sections (50 µm) cut following the completion of the experiment showing the extent of the CA3 cut along the septo-temporal axis. The extreme septal and temporal ends of the hippocampus are removed by the cut. Each micrograph is separated by approximately 1mm (shown on the left). **b:** raw data (0.1-500 Hz) local field potentials recorded from this preparation at the level indicated by the inset. Labeling was performed with Chicago Sky Blue (Sigma).



Nature Neuroscience: doi:10.1038/nn.2440

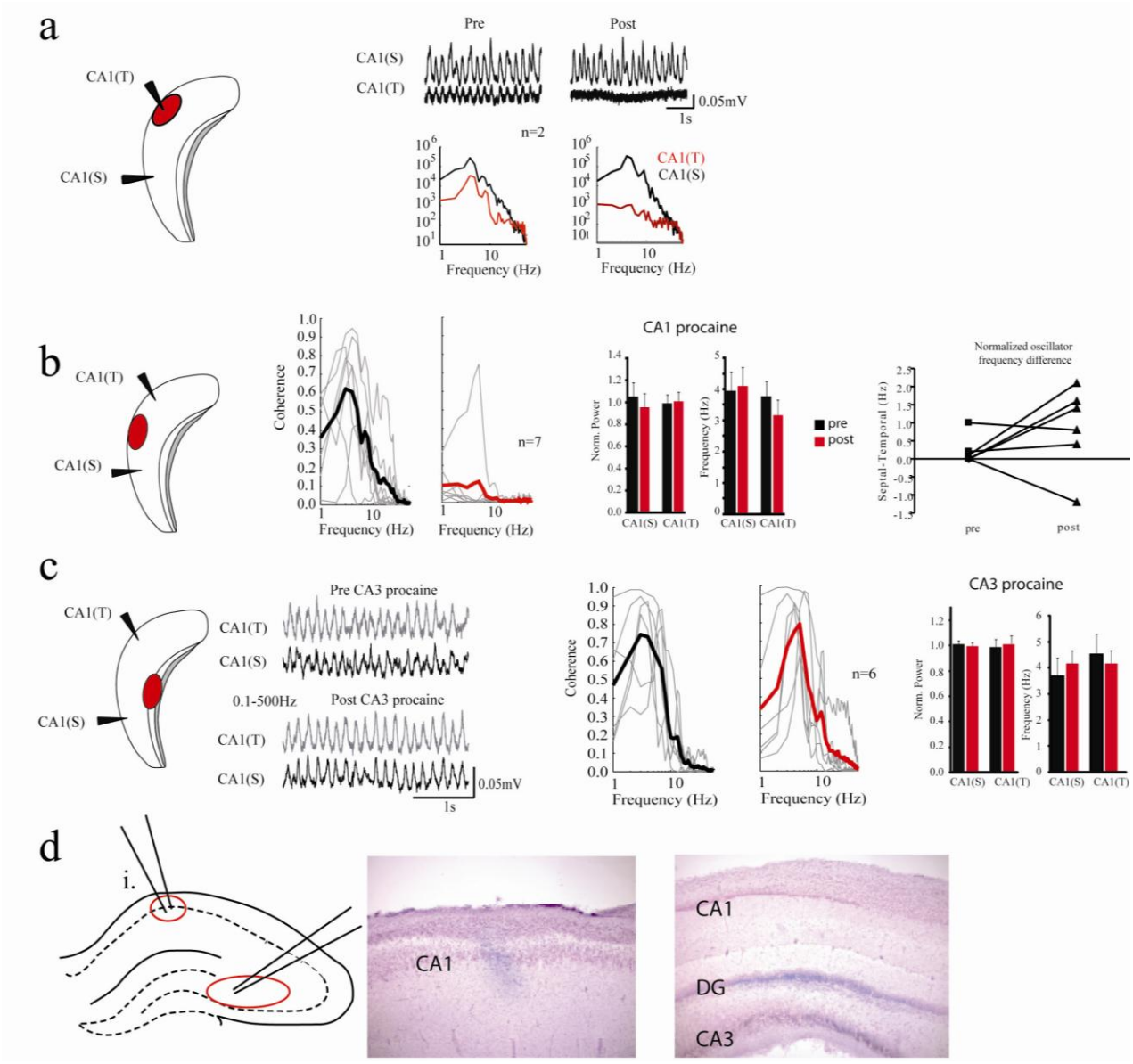


**Supplementary Figure 11: a:** Local procaine infusion abolishes hippocampal theta oscillation while leaving the opposing oscillator intact. The experimental paradigm is shown with the field recording electrode adjacent to the procaine cannula (red ellipse) in the temporal CA1 with the recording electrode in the septal CA1. On the right are the raw local field potentials and power spectrums from pre and post procaine showing an abolishment of theta in the recording site adjacent to the procaine cannula only. **b:** the paradigm used to demonstrate multiple hippocampal oscillators. Raw data from this experiment are shown in Fig. 2. The single cases of coherence between septal and temporal oscillators are shown along with the mean power and



Nature Neuroscience: doi:10.1038/nn.2440

theta frequency in the pre and post procaine conditions. Note that procaine in the middle hippocampus did not on average change the power or frequency of the septal or temporal oscillator. Note however, that the two regions were incoherent because they oscillated at two distinct frequencies (see main text). On the far right is the normalized frequency difference between the septal and temporal oscillator pre and post procaine. **c:** similar procaine injections into CA3 were without effect on intra CA1 coherence, frequency or power. Black lines and bars are pre procaine values and red lines and bars are post procaine values. **d:** histology demonstrating the location of the injection cannula in CA1 and CA3/DG.



Nature Neuroscience: doi:10.1038/nn.2440

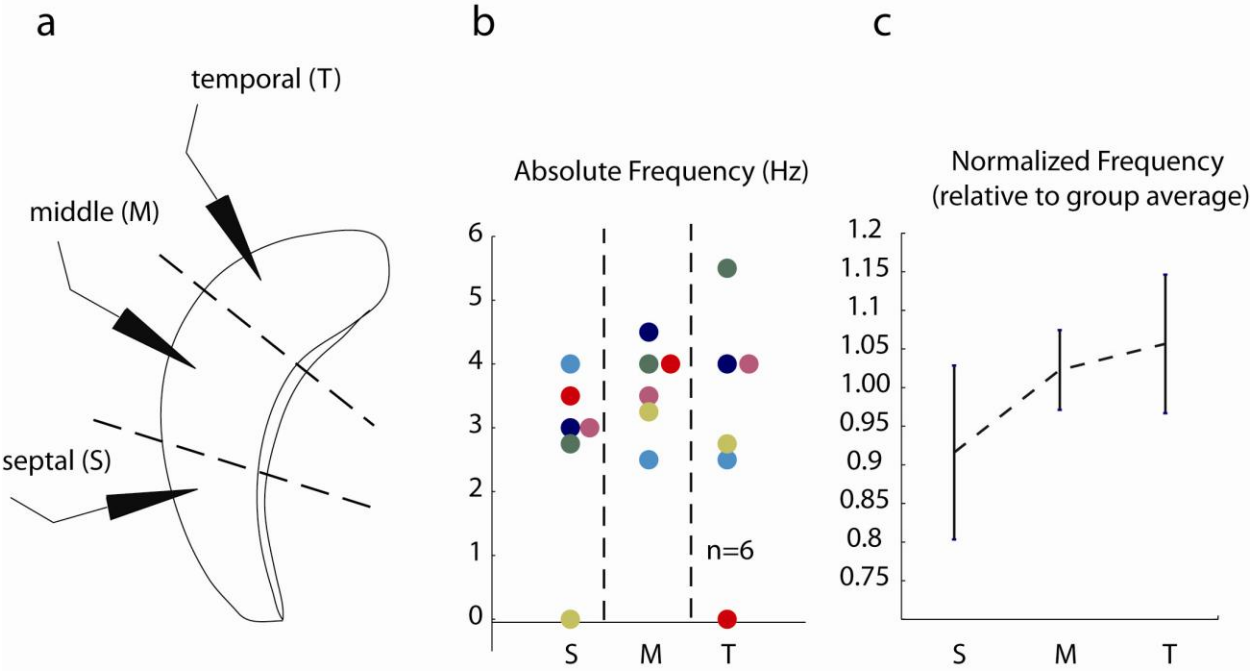


**Supplementary Figure 12:** Investigating the preferred oscillation frequencies of different regions of the hippocampus. **a:** The hippocampus was sectioned with a razor blade during the dissection procedure into the septal (s) middle (m) and temporal (t) segments and electrodes were placed in each region for 1hour to record the oscillatory activity. The peak frequency was taken as the average theta peak in the power spectrum from the recording period. **b:** plot of each experiment for the mean frequency of each region. **c:** normalized frequency plotted according to region. There was no systematic difference in mean frequency between regions although there was a trend for the frequency to increase in the septo-temporal direction. The value at 0 indicate that the region in that experiment did not oscillate.



Nature Neuroscience: doi:10.1038/nn.2440

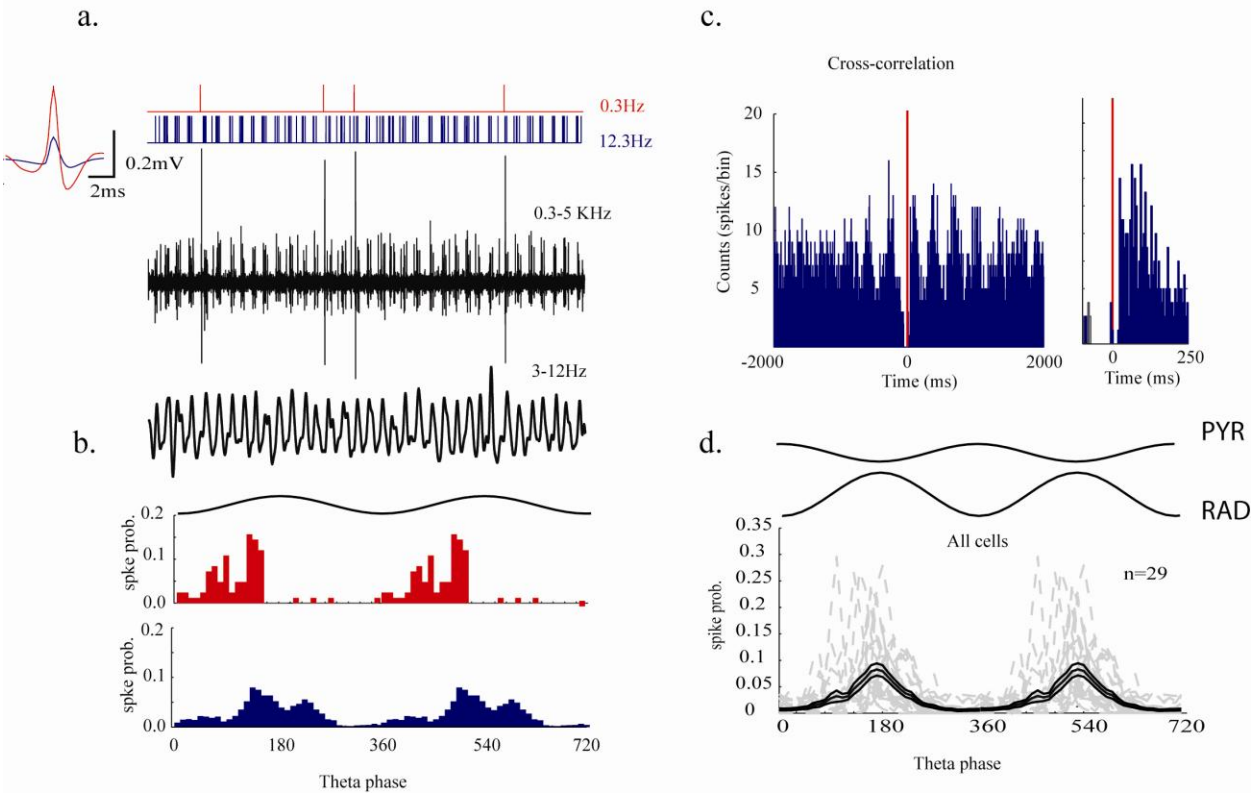


**Supplementary Figure 13: a:** Simultaneous extracellular recording of a putative principle cell (red) and non-principle cell interneuron (blue). Data were recorded from two electrodes, one recording field activity in stratum radiatum and the other spikes from the pyramidal cell layer. Two cells were apparent in this record (shown on the left) which differed mainly in spike height but also width. Raw data is shown in black and the spikes were detected and sorted using *wave_clus* semiautomatic spike sorting software[4]. The segment of raw data selected was from a period of high principle cell activity as the average was 0.3Hz. The detected spikes from the two cells are shown in red (principle cell) and blue (interneuron). **b**: The theta phase modulation of both cell types demonstrating the principle cell fires before the interneuron on the theta cycle. Bin width is 10º of the theta cycle. **c**: the cross correlation of the two cells using the principle cell as the reference demonstrates a theta (3.5Hz) periodicity in the period following the principle cell trigger (bin width is 5ms). On the right is an expanded view on the 300 ms around the principle cell spike showing an increase in spiking within 15 ms following principle cell discharge. **d**: The phase distribution of 29 single cell extracellular recordings showing that all cells fire near the peak of theta (from radiatum/ trough of theta from the other side of the phase reversal), although some variability is present on either side of the peak.



Nature Neuroscience: doi:10.1038/nn.2440

**Table 1:**

**Supplementary Table 1: Changes in relative theta power and frequency of the spontaneous oscillation recorded in the Str. radiatum of CA1 after the application of various antagonists of the cholinergic, GABAergic and glutamatergic transmission.**

| Antagonist | Relative theta power | | | Theta peak frequency | | |
|---|---|---|---|---|---|---|
| | Baseline | Antagonist | Wash | Baseline | Antagonist | Wash |
| Atropine (n=9, 10µM) | 1.03±0.05 | 0.94±0.12 | 1.29±0.18 | 6.25±0.6 | 5.75±0.6 | 5.65±0.5 |
| Tubocurarine (n=8, 10µM) | 1.04±0.04 | 1.02±0.28 | 0.95±0.09 | 4.62±0.7 | 4.25±0.8 | 4.12±0.5 |
| DNQX (n=6, 10µM) | 0.99±0.01 | **0.08±0.02*** ** | 0.88±0.11 | 5±1 | - | 4.17±0.65 |
| NBQX (n=5, 10µM) | 1.01±0.02 | **0.04±0.01*** ** | - | 7.4±1.12 | - | - |
| AP-V (n=5, 50µM) | 0.97±0.02 | 1.03±0.06 | 1.07±0.05 | 5±0.7 | **7.6±1.16*** | 4.6±0.7 |
| SYM2081 (n=7, 10µM) | 1.01±0.01 | 1.16±0.13 | 1.34±0.18 | 6.57±1.3 | 6.29±1.27 | 6.42±1.5 |
| MCPG (n=5, 200µM) | 1.04±0.04 | **0.64±0.1*** | 1.15±0.14 | 5.8±0.8 | 4.8±0.6 | 4.4±0.4 |
| Bicuculline (n=6, 5µM) | 1.06±0.02 | **0.13±0.05*** ** | 1.04±0.06 | 5.4±0.92 | - | 4.6±0.81 |
| CGP46381 (n=6, 10µM) | 1.02±0.03 | **0.61±0.14*** | 0.98±0.09 | 7.1±1.07 | 7.2±1.2 | 6±1.23 |



Nature Neuroscience: doi:10.1038/nn.2440

## Methods

**Dissection:** All procedures were performed according to protocols and guidelines approved by the McGill University Animal Care Committee and the Canadian Council on Animal Care. Sprague-Dawley rats (P15-28) were decapitated and the brain was rapidly removed from the skull and placed in ice cold high sucrose ACSF solution (in mM: 252 sucrose, 3 KCl, 2 MgSO4, 24 NaHCO3, 1.25 NaH2PO4, 1.2 CaCl2, and 10 glucose) and bubbled with carbogen (95%$O_2$ and 5%$CO_2$). A glass plate (inverted petri dish) covered with lens paper was used as the stage for the majority of the dissection. The glass plate can be rotated on the crushed ice throughout the dissection to gain access to various parts of the hippocampus with the dissection instruments. The cerebellum and frontal cortex were removed with a razor blade and the two hemispheres were separated and allowed to recover for 2-3 minutes in the oxygenated sucrose solution. The single hippocampal isolate was then removed from the remaining hemi-section in the following manner. One spatula supported the inner portion of the cortical hemisphere, and the other was used to gently pull away the brainstem and thalamus to expose the hippocampal artery and underlying CA3 and dentate gyrus (DG). To separate the hippocampus from the cortex the spatula was again placed between the cortex and extreme dorsal end of the hippocampus and moved smoothly through to the caudal portion of cortex. During this process the spatula helped separate the CA1/subicular tissue from the overlying cortex. The hippocampal complex was removed from the surrounding brain tissue by placing one spatula on the CA3/DG region of the dorsal hippocampus and pulling the dorsal hippocampus toward to the caudal portion of the brain. Blood vessels may impede prompt removal and should be cut away but not ripped out so as to avoid unnecessary tissue damage. The entire hippocampal isolation procedure was completed within 1 minute. Any remaining cortex was removed using micro-scissors when the



Nature Neuroscience: doi:10.1038/nn.2440

preparation was returned to the oxygenated sucrose solution. Following dissection the hippocampal complex was left at room temperature in ACSF bubbled with carbogen for 45-180 minutes. For recording, the preparation was transferred quickly to the custom submerged recording chamber. In the experiments where CA3 was removed, a thin razor blade was placed through the septo-temporal extent of the entire hippocampus at an angle to remove CA3 inputs to CA1 (see supplementary figure 10). This procedure also removed the most extreme septal and temporal ends of CA1. Following the completion of the experiment the strip of CA3 and CA1/subiculum were fixed and cut as described below. Procaine hydrochloride experiments were performed using a 30 gauge needle attached to a Hamilton syringe. Procaine (0.1-1µL; 20% with Chicago Sky Blue) was infused into the region of interest after 5-10 minutes of baseline data collection. The larger infusions (0.5-1µL) were used in the CA3 inactivation experiments.

**Data Recording and Analysis:**

For recording, the preparation was continuously perfused with aCSF (25ml/min, in mM: 126 NaCl, 24 NaHCO3, 10glucose, 3.5-5 KCl, 2 MgSO4, 1.25 NaH2PO4, and 2 CaCl2 ; pH 7.4, with 95%O2/5% CO2) via a gravity fed perfusion system and maintained at 30-32ºC. The majority of the experiments used a KCl concentration of 4-4.5 mM (see Supplementary figure 7). Local field potentials were recorded using glass micropipettes (1-4MΩ) filled with aCSF. Signals were recorded a differential AC amplifier (AM systems), filtered online (0.1-500 Hz) and sampled at 5-10KHz. Signal were referenced to the bath medium and connected to ground. Extracellular single units were recorded using the same pipettes; putative interneurons and pyramidal neurons were differentiated based in part on previously reported properties [5] of these neurons, where pyramidal cells have a slow firing rate (<1 Hz) and large spike width (peak to



Nature Neuroscience: doi:10.1038/nn.2440

trough of ≥1 ms) whereas interneurons have a more narrow spike width and a faster firing rate (up to 20 Hz).

Whole cell recordings were performed using the blind patch technique as described previously [6]. Briefly, pipettes were pulled using borosilicate glass with a resistance of 3-8MΩ when filled with 144 K-gluconate, 3 MgCl2,0.2 EGTA, 10 HEPES, 2 ATP, and 0.3 GTP, pH 7.2 (285–295 mOsm). Recordings were performed using a patch-clamp amplifier PC-505A (Warner Instruments, Hamden,CT). Cell characterization was performed by injecting (0-100 pA), 2 s long, depolarizing and hyperpolarizing current steps. Principle cell – interneuron differentiation was made using spike width (mean principle cells = 3.2 ± 0.1ms; mean interneurons = 1.5 ± 0.1ms). Spike frequency estimation was confounded by the extracellular oscillation although interneurons and principle cells also maintained differences in spike frequency adaptation and firing rate. In addition some neurons were identified using Neurobiotin (0.1-0.5 %) in the recording pipette using the protocol described by [7]. Recordings were not corrected for the junction potential (9 mV).

**Data Analysis:** Local field potentials were down sampled and filtered to 500Hz, and the first and last second of data removed. Filtering was performed in the forward and reverse direction to eliminate phase distortions. Power spectrums were calculated using the Welch method by averaging 2-5s periodgrams with a 50% overlap between segments. Mean squared coherence (Cxy=Pxy/sqrt(Pxx.Pyy)) between two electrodes was assessed using the same size window and where Pxy is the cross spectrum and Pxx and Pyy are the individual power spectrums. Coherence significance was computed by shifting one signal 100 times by a random time interval in either the positive or negative direction. The mean randomized coherence value + 2 standard deviations



Nature Neuroscience: doi:10.1038/nn.2440

was considered the 95% confidence interval. The significance of autocorrelations were calculated using the autocorrelation of 100 segments of filtered white noise and the 95% confidence interval was calculated using the mean + 2 standard deviation of this surrogate set. Significant peaks above this value were taken as a sign of periodicity in the signal. Current source density was calculated using the formula: CSD = $([f(_{pi-1}) - 2f(_{pi}) + f(_{pi-1})]/d2$, where $f_{pi}$ is the averaged theta waveform recorded from depth *i*, and *d* is the distance between steps (75µm). An electrode from nearby recorded stratum radiatum (<1 mm) was used as a reference to collect data triggered by the theta peak of 100, 1.5s traces. These traces were averaged and inserted into the CSD algorithm. Therefore every level used for the averaged CSD analysis was a theta peak triggered average.

To determine the neurotransmitters and receptors involved in these intrinsic theta oscillations, we bath applied antagonists targeting cholinergic, GABAergic and glutamatergic neurotransmission. For this purpose, we computed the power (in $\mu V^2$ / Hz) at peak frequency of 2 seconds of data during baseline, drug application and washout. To obtain numerical values, power of the theta band (3-10 Hz) and peak frequency was averaged from a 2 min recording for each condition (baseline, last two minutes of drug application and washout). The whole cell recorded data were analyzed using pClamp 10.0 for calculation of spike width, sag, AHP and firing frequency. The relationship between membrane potential and the local field was calculated with Spike2 or Matlab.

**Statistical Analysis:** All statistical analyses were carried out in Graphpad. Analysis of variance (ANOVA) with repeated measures was used to compute the difference between means. Post-hoc ANOVAs were used to verify specific hypotheses and were corrected with the Bonferroni



Nature Neuroscience: doi:10.1038/nn.2440

method. All data are expressed as mean ± standard error of the mean (s.e.m), unless otherwise indicated.

**Histology:** Following completion of the experiment, hippocampi were fixed in 4% paraformaldehyde followed by sucrose until saturated. Tissue was cut (50 µm) at -20ºC with a cryostat to visualize the electrode placement, the position of cannulas, and blue dye used in the procaine experiments. The tissue was cut either in the coronal or horizontal orientation, mounted on gelatine coated slides, and stained with cresyl violet or fast red.

## Discussion:

The results presented here have shown that the hippocampus generates theta oscillation intrinsically without afferent input. This intrahippocampal theta network arises from mutual coupling of many individual theta oscillators organized along the septotemporal axis of the proximal CA1. The oscillation is present without input from CA3 suggesting local principle cell-interneuron excitation gives rise to widespread feedback inhibition to the large principle cell population which consequently phase modulates the timing of subsequent principle cell spiking. With this model, only a small number of principle cells are required to spike at any cycle due to the ratio of principle cells to interneurons and because the efficacy of the principle cell-interneuron synapses[8, 9]. In this manner a small level of excitation can give rise to enormous network wide inhibition.

### Previous *in vitro* studies

Previous *in vitro* studies using hippocampal slices have likely lacked the circuitry necessary to observe this network theta rhythm. We found this was the case in small number of slices that we



Nature Neuroscience: doi:10.1038/nn.2440

tested under identical experimental conditions. There have been previous reports of slow spontaneous activity in the whole hippocampus or ventral hippocampal slices, however a number of methodological differences may account for the type of activity observed in those experiments [10-13]. Many models of *in vitro* theta activity have been described, although the mechanisms by which theta arises with these protocols must be considered in the context of how closely the model mimics the actual phenomena. The carbachol model of hippocampal theta[14-17] does not require GABAergic inhibition and is accompanied by synchronous bursting from CA3 neurons. *In vivo* theta does require GABAergic inhibition and CA3 cells do not fire every theta cycle in bursts (except during phase precession, which is likely cortically mediated). Moreover, the presence of theta activity in the freely moving animal does not require cholinergic neurons[18] or muscarinic receptor activation[19]. However, the aforementioned model does serve an important function for investigating other rhythms such as gamma, as well as for studying rhythm switching within local networks.

The anatomical complexity of the hippocampus does not lend itself to slice preparations for the study of network interactions[20]. The intact hippocampus will maintain the integrity of all intrinsic networks, but specifically the wide branching horizontally oriented interneurons which are most likely damaged in any slice preparation[21]. Furthermore, the number of principle cells may also be of importance as a sparsely firing principle cell population may not be sufficient to consistently excite interneurons in slice preparations. The intrinsic hippocampal theta oscillator seems to function in the septotemporal axis, in accordance with the theta networks described previously[22].

**Comparison with *in vivo* data**



Nature Neuroscience: doi:10.1038/nn.2440

We show that intrinsic circuitry gives rise to a self organized form of theta rhythm when isolated from all afferent inputs. We do not claim however that theta activity *in vivo* is entirely intrinsic, as known inputs from CA3 and the entorhinal cortex generate substantial current sinks within stratum radiatum and the lacunosum molecular layer. Indeed, the intrinsic hippocampal theta oscillation reported here differs from *in vivo* data in the amplitude, and current source density. The amplitude of the intrinsic theta rhythm was typically 10-20% of *in vivo* values (likely due to a lack of medial septal and entorhinal input). Moreover, the current source density *in vivo* shows multiple phase shifted theta dipoles[23] corresponding to discrete layer specific input from entorhinal layer III and CA3. In our data we found a single dipole which seems to originate mainly from the subthreshold oscillations of large groups of neurons in the cell layer. This CSD profile is somewhat similar to that shown in Bragin et al., (1995) following bilateral removal of the entorhinal cortex.

The necessity of the medial septum in theta generation has dominated the literature. The data presented here do not necessarily contradict previous experimental reports using temporary medial septal inactivation given that many studies report residual theta following lesion. Almost all studies using inactivation or lesion of the medial septum have suggested that these manipulations abolish theta [24-32]. These studies arrive at this conclusion based on the reduction in hippocampal theta power, whereas the periodicity of the field potentials is rarely quantified. Furthermore, many studies have indicated the presence of residual theta activity in the form of field potentials[27] and single units[30]. The remaining hippocampal theta is typically suggested to arise from remaining fibers not affected by the lesion. The most striking conclusion drawn from these collection of papers is that it is difficult to abolish hippocampal theta rhythm periodicity[26]. We therefore suggest that when the medial septal inputs are removed, the remaining (small



Nature Neuroscience: doi:10.1038/nn.2440

amplitude) theta could arise from intrinsic hippocampal circuits. However, future studies using more temporally specific inactivation techniques will allow a more precise illumination of how certain cells control the features of hippocampal theta rhythms.



Nature Neuroscience: doi:10.1038/nn.2440

Supplementary References

1. Jackson, J., Dickson, C.T. & Bland, B.H. Median raphe stimulation disrupts hippocampal theta via rapid inhibition and state-dependent phase reset of theta-related neural circuitry. *J Neurophysiol* **99**, 3009-3026 (2008).
2. Jackson, J., Young, C.K., Hu, B. & Bland, B.H. High frequency stimulation of the posterior hypothalamic nucleus restores movement and reinstates hippocampal-striatal theta coherence following haloperidol-induced catalepsy. *Exp Neurol* **213**, 210-219 (2008).
3. McNay, E.C. & Sherwin, R.S. From artificial cerebro-spinal fluid (aCSF) to artificial extracellular fluid (aECF): microdialysis perfusate composition effects on in vivo brain ECF glucose measurements. *J Neurosci Methods* **132**, 35-43 (2004).
4. Quiroga, R.Q., Nadasdy, Z. & Ben-Shaul, Y. Unsupervised spike detection and sorting with wavelets and superparamagnetic clustering. *Neural Comput* **16**, 1661-1687 (2004).
5. Csicsvari, J., Hirase, H., Czurko, A., Mamiya, A. & Buzsaki, G. Oscillatory coupling of hippocampal pyramidal cells and interneurons in the behaving Rat. *J Neurosci* **19**, 274-287 (1999).
6. Manseau, F., Goutagny, R., Danik, M. & Williams, S. The hippocamposeptal pathway generates rhythmic firing of GABAergic neurons in the medial septum and diagonal bands: an investigation using a complete septohippocampal preparation in vitro. *J Neurosci* **28**, 4096-4107 (2008).
7. Glickfeld, L.L., Roberts, J.D., Somogyi, P. & Scanziani, M. Interneurons hyperpolarize pyramidal cells along their entire somatodendritic axis. *Nat Neurosci* **12**, 21-23 (2009).
8. Csicsvari, J., Hirase, H., Czurko, A. & Buzsaki, G. Reliability and state dependence of pyramidal cell-interneuron synapses in the hippocampus: an ensemble approach in the behaving rat. *Neuron* **21**, 179-189 (1998).
9. Gulyas, A.I*., et al.* Hippocampal pyramidal cells excite inhibitory neurons through a single release site. *Nature* **366**, 683-687 (1993).
10. Colgin, L.L*., et al.* Spontaneous waves in the dentate gyrus of slices from the ventral hippocampus. *J Neurophysiol* **92**, 3385-3398 (2004).
11. Maier, N., Nimmrich, V. & Draguhn, A. Cellular and network mechanisms underlying spontaneous sharp wave-ripple complexes in mouse hippocampal slices. *J Physiol* **550**, 873-887 (2003).
12. Papatheodoropoulos, C., Sotiriou, E., Kotzadimitriou, D. & Drimala, P. At clinically relevant concentrations the anaesthetic/amnesic thiopental but not the anticonvulsant phenobarbital interferes with hippocampal sharp wave-ripple complexes. *BMC Neurosci* **8**, 60 (2007).
13. Wu, C., Shen, H., Luk, W.P. & Zhang, L. A fundamental oscillatory state of isolated rodent hippocampus. *J Physiol* **540**, 509-527 (2002).
14. Konopacki, J., Bland, B.H. & Roth, S.H. Phase shifting of CA1 and dentate EEG theta rhythms in hippocampal formation slices. *Brain Res* **417**, 399-402 (1987).
15. Konopacki, J., MacIver, M.B., Bland, B.H. & Roth, S.H. Carbachol-induced EEG 'theta' activity in hippocampal brain slices. *Brain Res* **405**, 196-198 (1987).
16. MacVicar, B.A. & Tse, F.W. Local neuronal circuitry underlying cholinergic rhythmical slow activity in CA3 area of rat hippocampal slices. *J Physiol* **417**, 197-212 (1989).
17. Williams, J.H. & Kauer, J.A. Properties of carbachol-induced oscillatory activity in rat hippocampus. *J Neurophysiol* **78**, 2631-2640 (1997).
18. Lee, M.G., Chrobak, J.J., Sik, A., Wiley, R.G. & Buzsaki, G. Hippocampal theta activity following selective lesion of the septal cholinergic system. *Neuroscience* **62**, 1033-1047 (1994).



Nature Neuroscience: doi:10.1038/nn.2440

19. Kramis, R., Vanderwolf, C.H. & Bland, B.H. Two types of hippocampal rhythmical slow activity in both the rabbit and the rat: relations to behavior and effects of atropine, diethyl ether, urethane, and pentobarbital. *Exp Neurol* **49**, 58-85 (1975).
20. Amaral, D.G. & Witter, M.P. The three-dimensional organization of the hippocampal formation: a review of anatomical data. *Neuroscience* **31**, 571-591 (1989).
21. Maccaferri, G. Stratum oriens horizontal interneurone diversity and hippocampal network dynamics. *J Physiol* **562**, 73-80 (2005).
22. Gloveli, T.*, et al.* Orthogonal arrangement of rhythm-generating microcircuits in the hippocampus. *Proc Natl Acad Sci U S A* **102**, 13295-13300 (2005).
23. Bragin, A.*, et al.* Gamma (40-100 Hz) oscillation in the hippocampus of the behaving rat. *J Neurosci* **15**, 47-60 (1995).
24. Andersen, P., Bland, H.B., Myhrer, T. & Schwartzkroin, P.A. Septo-hippocampal pathway necessary for dentate theta production. *Brain Res* **165**, 13-22 (1979).
25. Givens, B. & Olton, D.S. Local modulation of basal forebrain: effects on working and reference memory. *J Neurosci* **14**, 3578-3587 (1994).
26. Gray, J.A. Medial septal lesions, hippocampal theta rhythm and the control of vibrissal movement in the freely moving rat. *Electroencephalogr Clin Neurophysiol* **30**, 189-197 (1971).
27. Kirk, I.J. & McNaughton, N. Mapping the differential effects of procaine on frequency and amplitude of reticularly elicited hippocampal rhythmical slow activity. *Hippocampus* **3**, 517-525 (1993).
28. Lawson, V.H. & Bland, B.H. The role of the septohippocampal pathway in the regulation of hippocampal field activity and behavior: analysis by the intraseptal microinfusion of carbachol, atropine, and procaine. *Exp Neurol* **120**, 132-144 (1993).
29. Leung, L.S., Martin, L.A. & Stewart, D.J. Hippocampal theta rhythm in behaving rats following ibotenic acid lesion of the septum. *Hippocampus* **4**, 136-147 (1994).
30. Leutgeb, S. & Mizumori, S.J. Excitotoxic septal lesions result in spatial memory deficits and altered flexibility of hippocampal single-unit representations. *J Neurosci* **19**, 6661-6672 (1999).
31. Mitchell, S.J., Rawlins, J.N., Steward, O. & Olton, D.S. Medial septal area lesions disrupt theta rhythm and cholinergic staining in medial entorhinal cortex and produce impaired radial arm maze behavior in rats. *J Neurosci* **2**, 292-302 (1982).
32. Yoder, R.M. & Pang, K.C. Involvement of GABAergic and cholinergic medial septal neurons in hippocampal theta rhythm. *Hippocampus* **15**, 381-392 (2005).



Nature Neuroscience: doi:10.1038/nn.2440